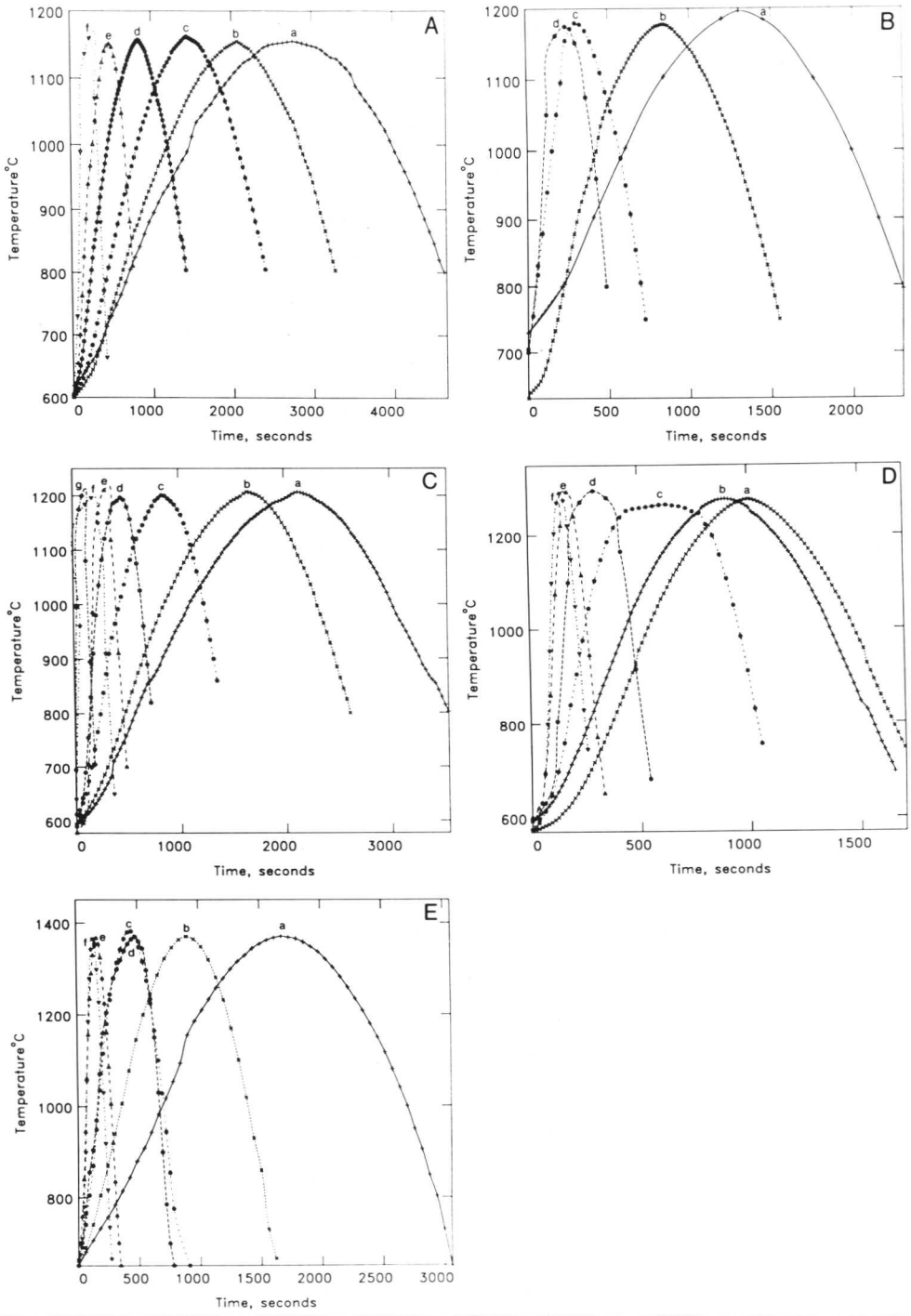

Figure 6.4. Temperature (°C) versus time (s) graphs plotted after zone annealing MA956 at the temperatures ranging from 1150 to 1380°C,

Figure	T_p	Profiles	Specimen travel speeds mm/min
6.4A	1150°C	a-f	0.2, 0.4, 0.8, 1.4, 3.2 and 5.0
6.4B	1180°C	a-d	0.8, 1.4, 3.2 and 5.0
6.4C	1200°C	a-g	0.4, 0.8, 1.4, 3.2, 5.0, 7.7 and 10.0
6.4D	1280°C	a-f	0.8, 1.4, 3.2, 5.0, 7.7 and 10.0
6.4E	1380°C	a-f	0.8, 1.4, 3.2, 5.0, 7.7 and 10.0

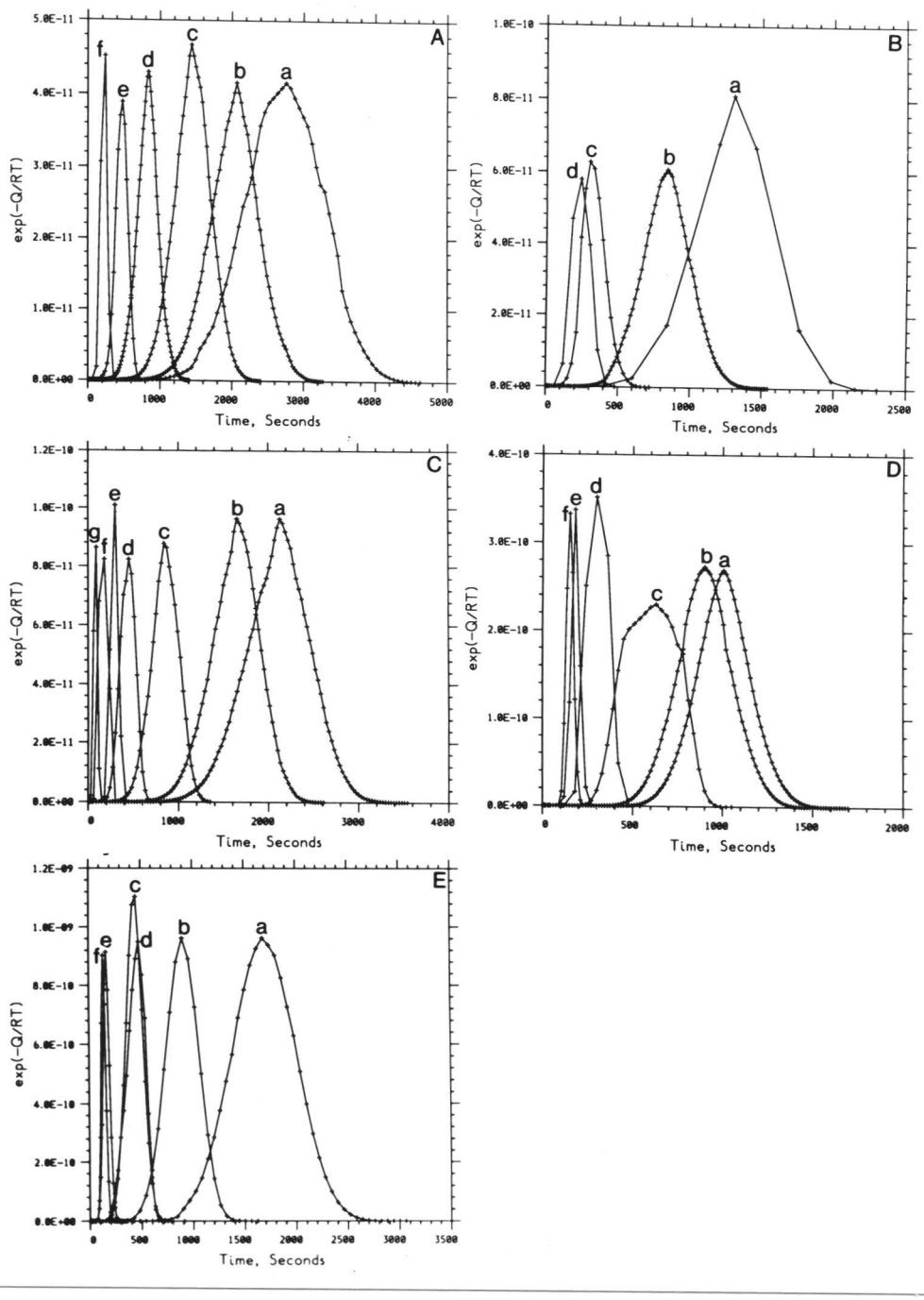

Figure 6.5. Graphs of exp(-Q/RT) versus time in seconds. The area under each curve is a measure of kinetic strength.

Figure	T_p	Profiles	Specimen travel speeds mm/min
6.4A	1150°C	a-f	0.2, 0.4, 0.8, 1.4, 3.2 and 5.0
6.4B	1180°C	a-d	0.8, 1.4, 3.2 and 5.0
6.4C	1200°C	a-g	0.4, 0.8, 1.4, 3.2, 5.0, 7.7 and 10.0
6.4D	1280°C	a-f	0.8, 1.4, 3.2, 5.0, 7.7 and 10.0
6.4E	1380°C	a-f	0.8, 1.4, 3.2, 5.0, 7.7 and 10.0

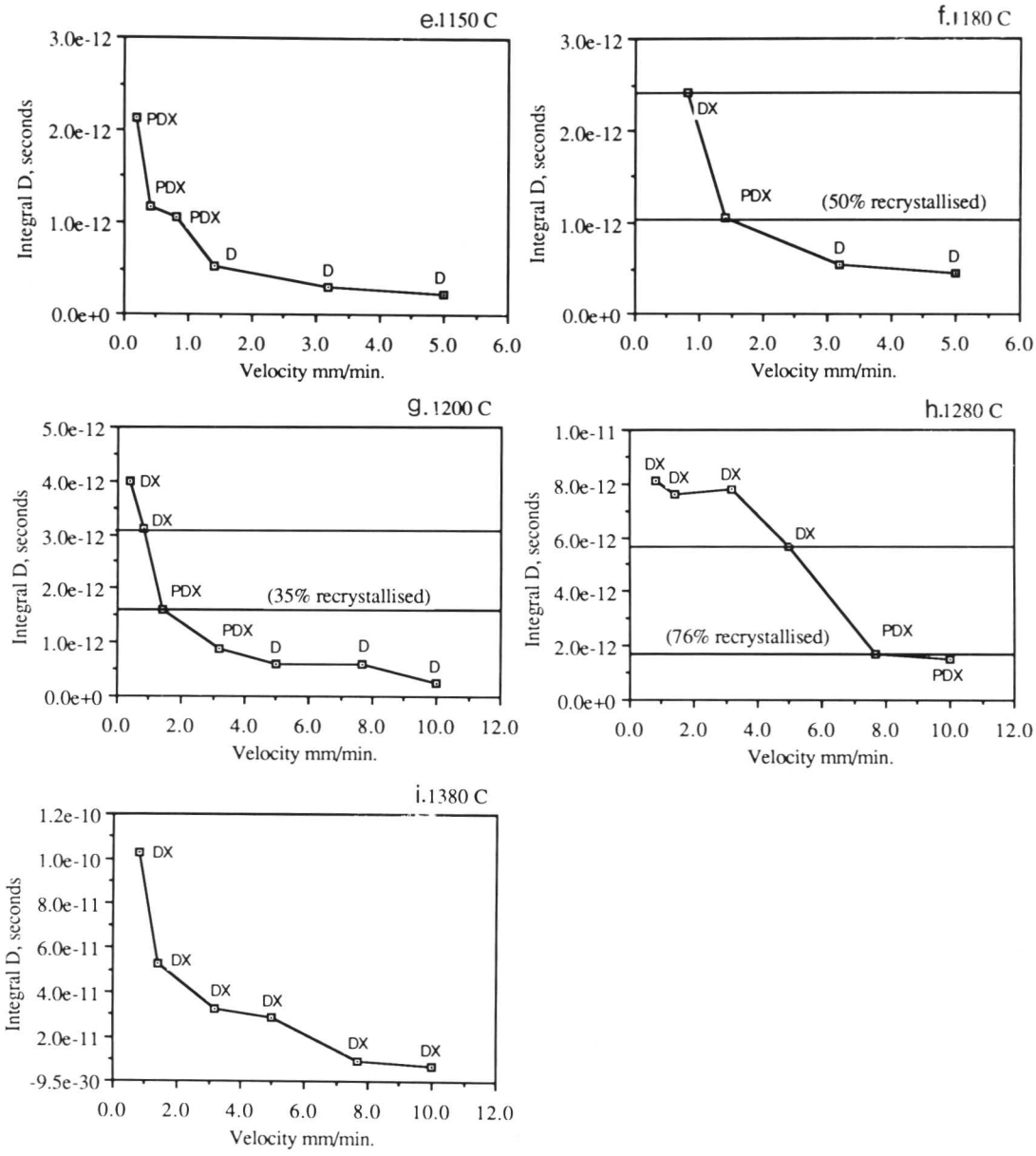

Figure 6.6. Showing the graphs plotted for Integral D (seconds) versus velocity, mm min^{-1}. Graphs e-h were plotted using the measured value of Q (402791 J mol^{-1}).

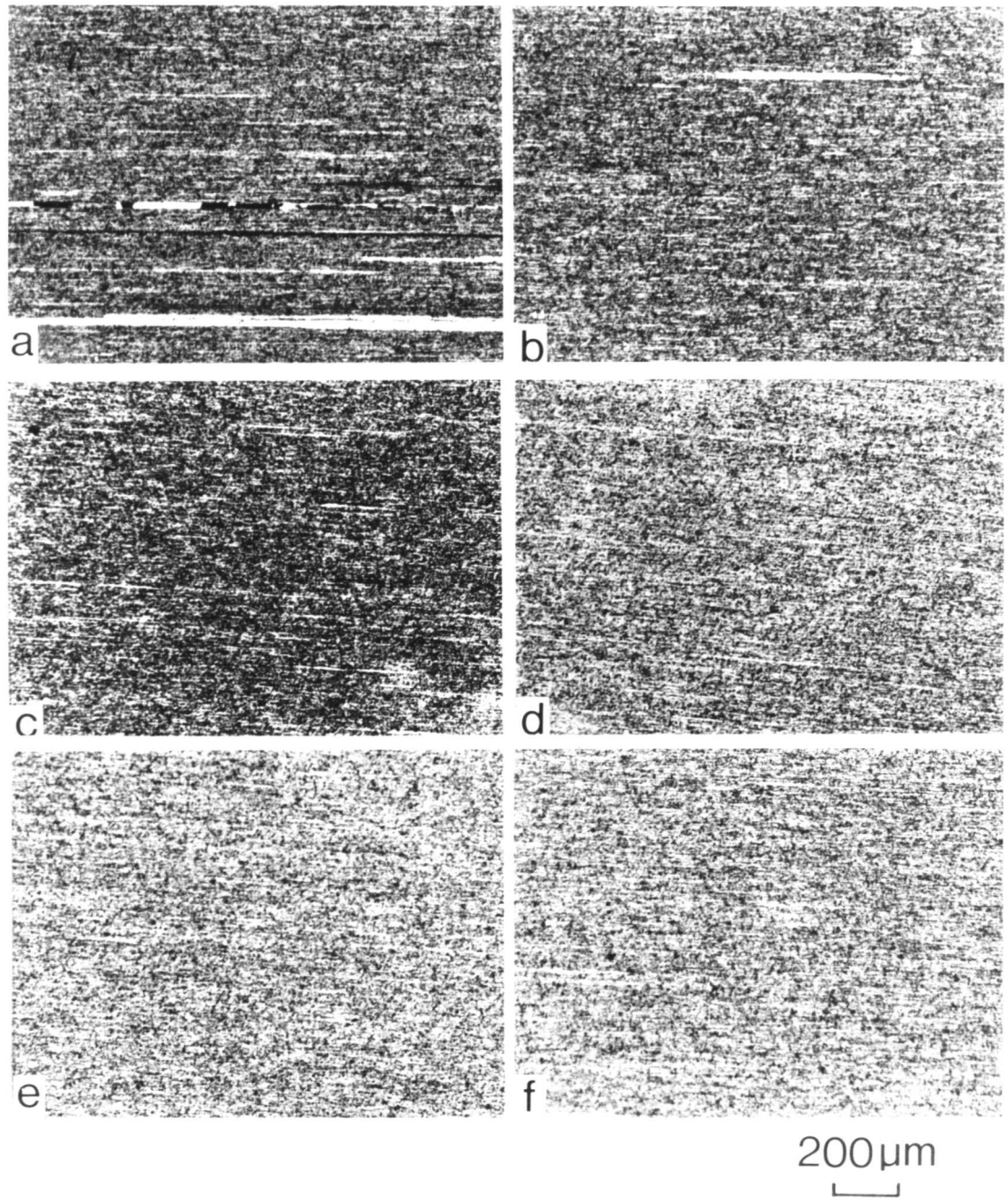

Figure 6.7. Optical micrographs recorded after zone annealing specimens at T_p = 1150°C. The micrographs are from the regions where T_p was measured.

a. Specimen travel speed 0.2 mm/min b. Specimen travel speed 0.4 mm/min

c. Specimen travel speed 0.8 mm/min d. Specimen travel speed 1.4 mm/min

e. Specimen travel speed 3.2 mm/min f. Specimen travel speed 5.0 mm/min

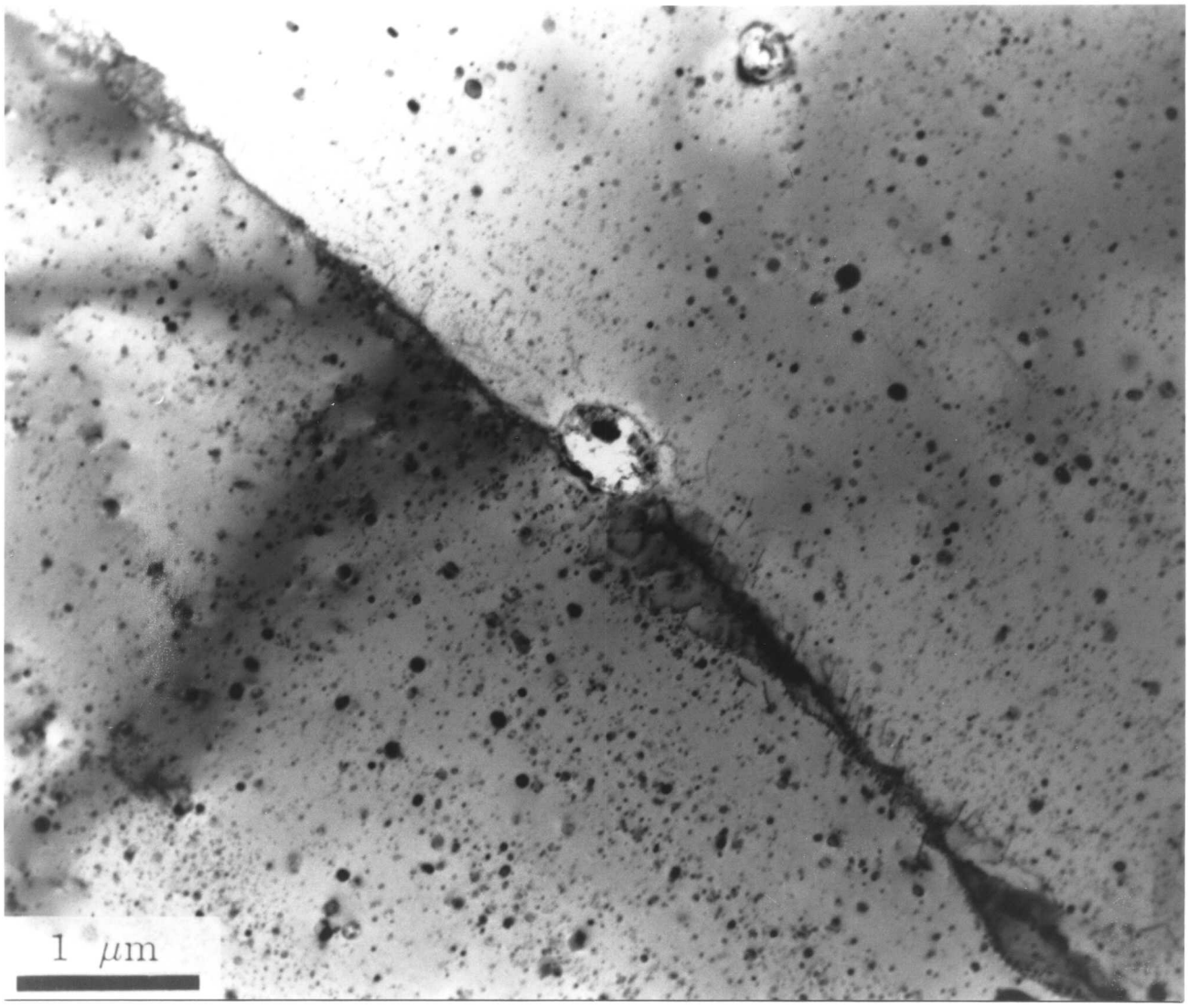

Figure 6.10. Transmission electron micrograph recorded using a foil prepared from the longitudinal section of the sample zone annealed with T_p = 1180°C and a specimen travel speed of 0.8 mm/min. Note the alignment of the particles and the fact that the grain boundary trace is parallel to the rows of particles.

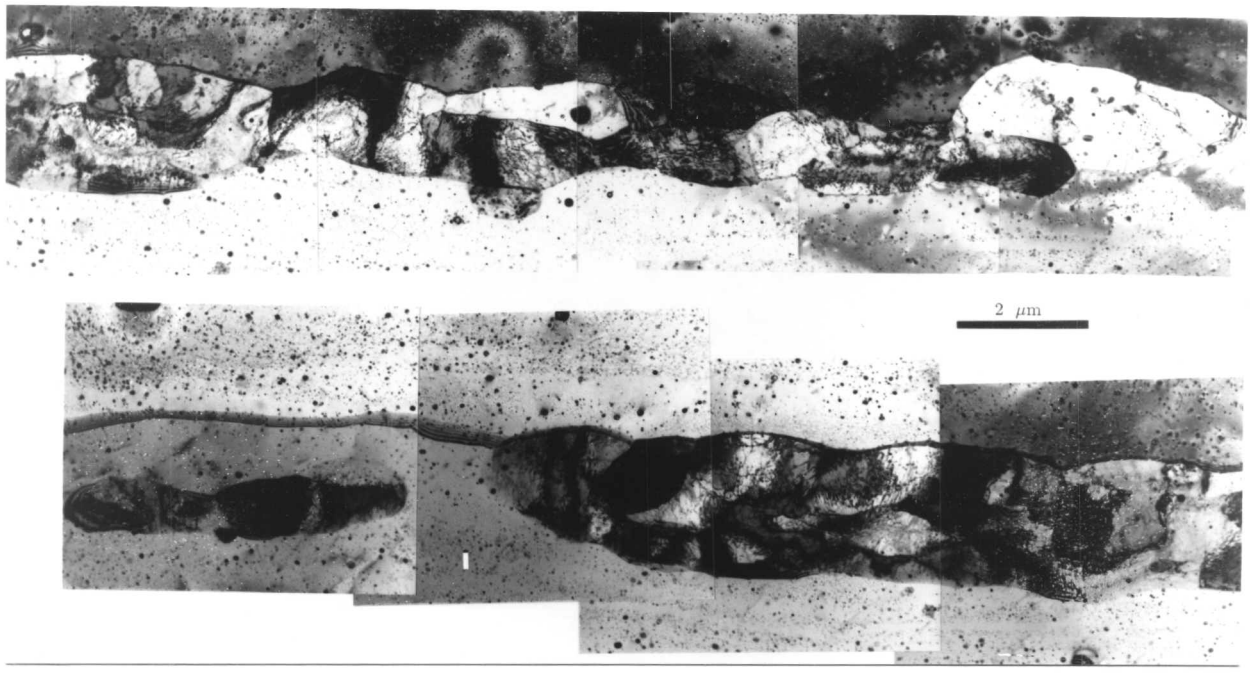

Figure 6.11. Transmission electron micrographs of the samples zone annealed at 1280°C at a specimen travel speed of 3.2 mm/min. Streams of unrecrystallised grains are seen to be trapped between two fully recrystallised, "dislocation free" grains.

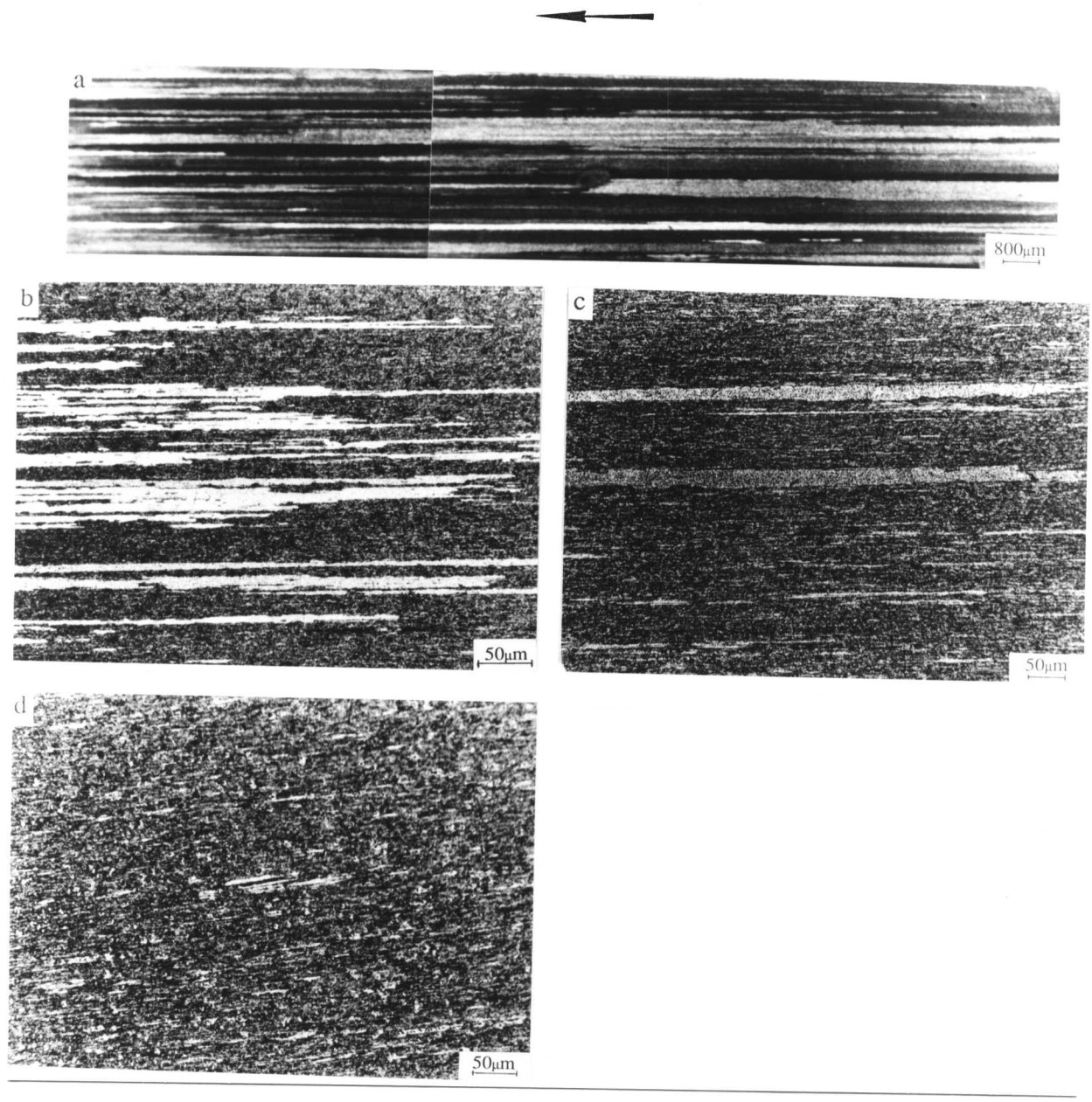

Figure 6.8. Optical micrographs recorded after zone annealing specimens at 1180°C. The arrow indicates the rolling and zone annealing direction.

a. Specimen travel speed 0.8 mm/min b. Specimen travel speed 1.4 mm/min

c. Specimen travel speed 3.2 mm/min d. Specimen travel speed 5.0 mm/min

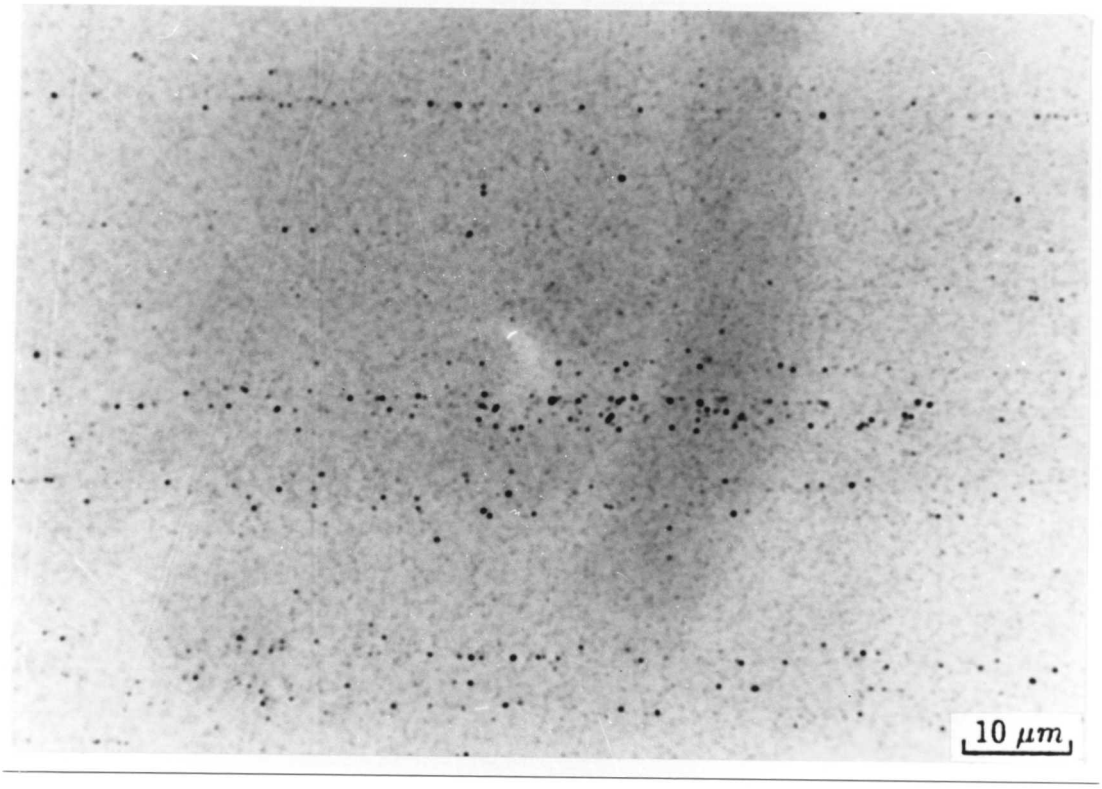

Figure 6.9. Showing alignment of particles along the rolling direction, recorded from an unetched sample of MA956.

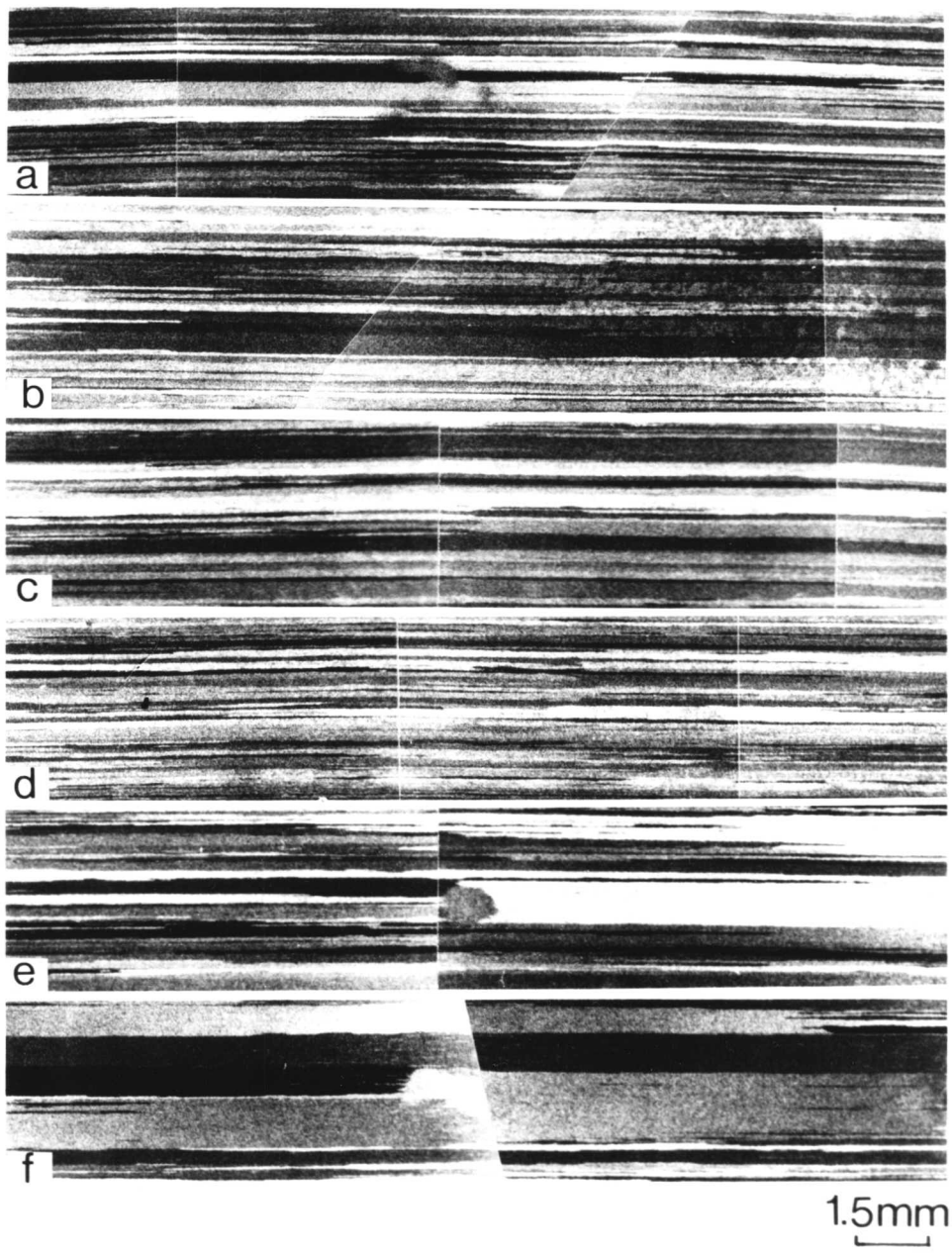

Figure 6.12. Optical micrographs recorded after zone annealing MA956 at T_p = 1280°C. The arrow indicates the direction of zone annealing.

a. 0.8 mm/min b. 1.4 mm/min c. 3.2 mm/min

d. 5.0 mm/min e. 7.7 mm/min f. 10.0 mm/min

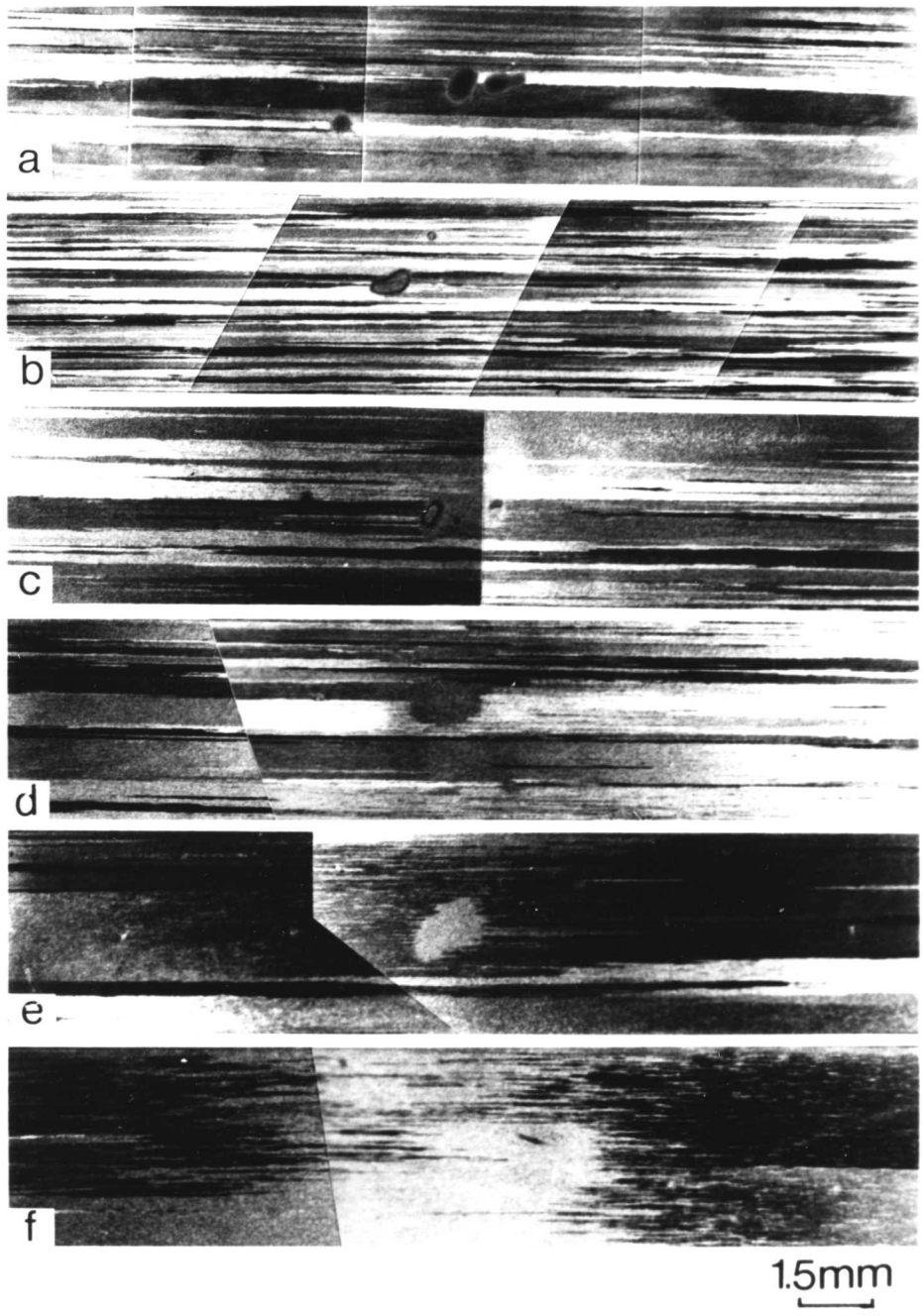

Figure 6.13. Optical micrographs recorded after zone annealing MA956 at T_p = 1380°C,

a. 0.8 mm/min b. 1.4 mm/min c. 3.2 mm/min

d. 5.0 mm/min e. 7.7 mm/min f. 10.0 mm/min

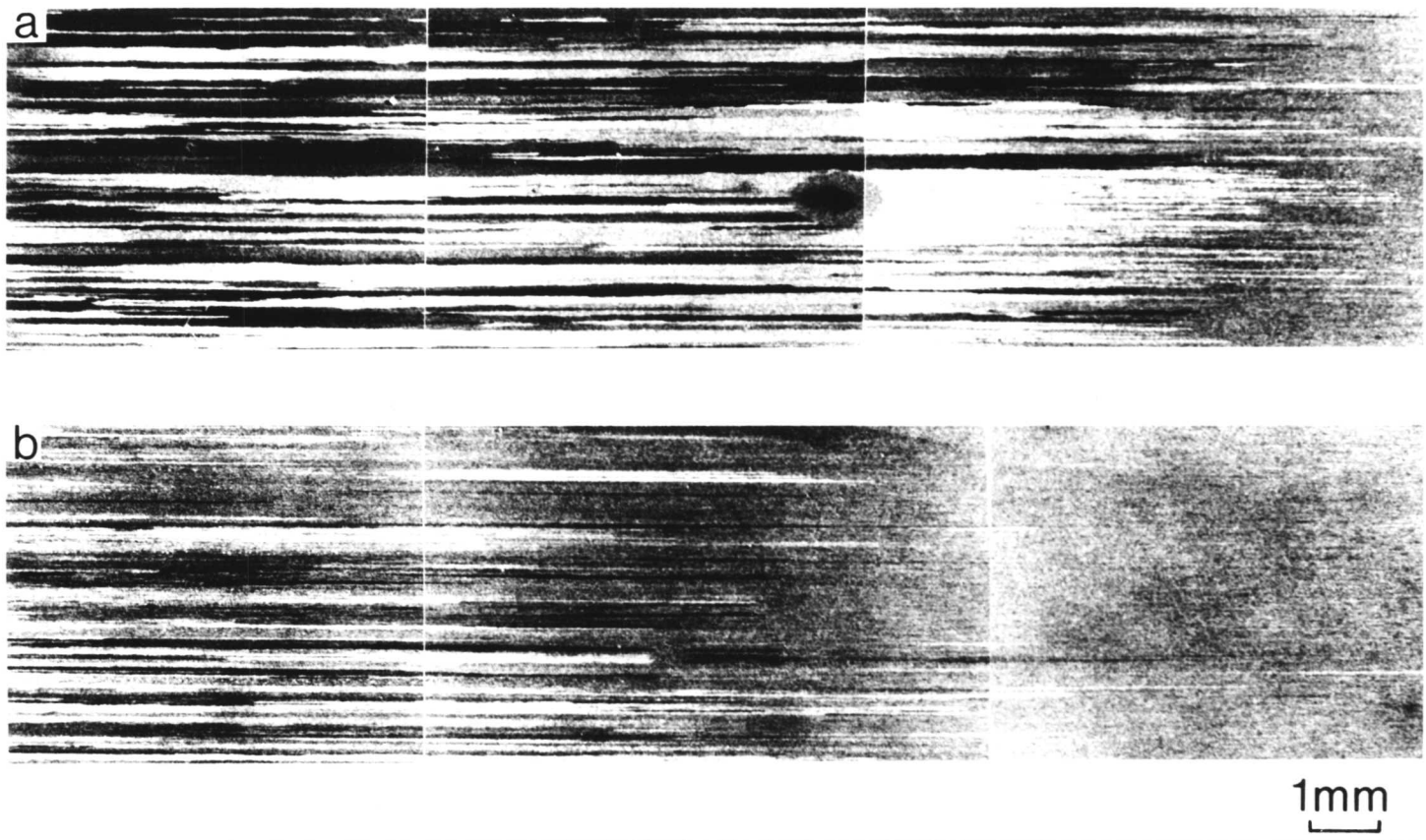

Figure 6.14. Optical micrographs recorded after zone annealing MA956 at T_p = 1280°C, but with the specimens rapidly quenched in water after partial passage through the R. F. coil.

a. 0.8 mm/min b. 7.7 mm/min

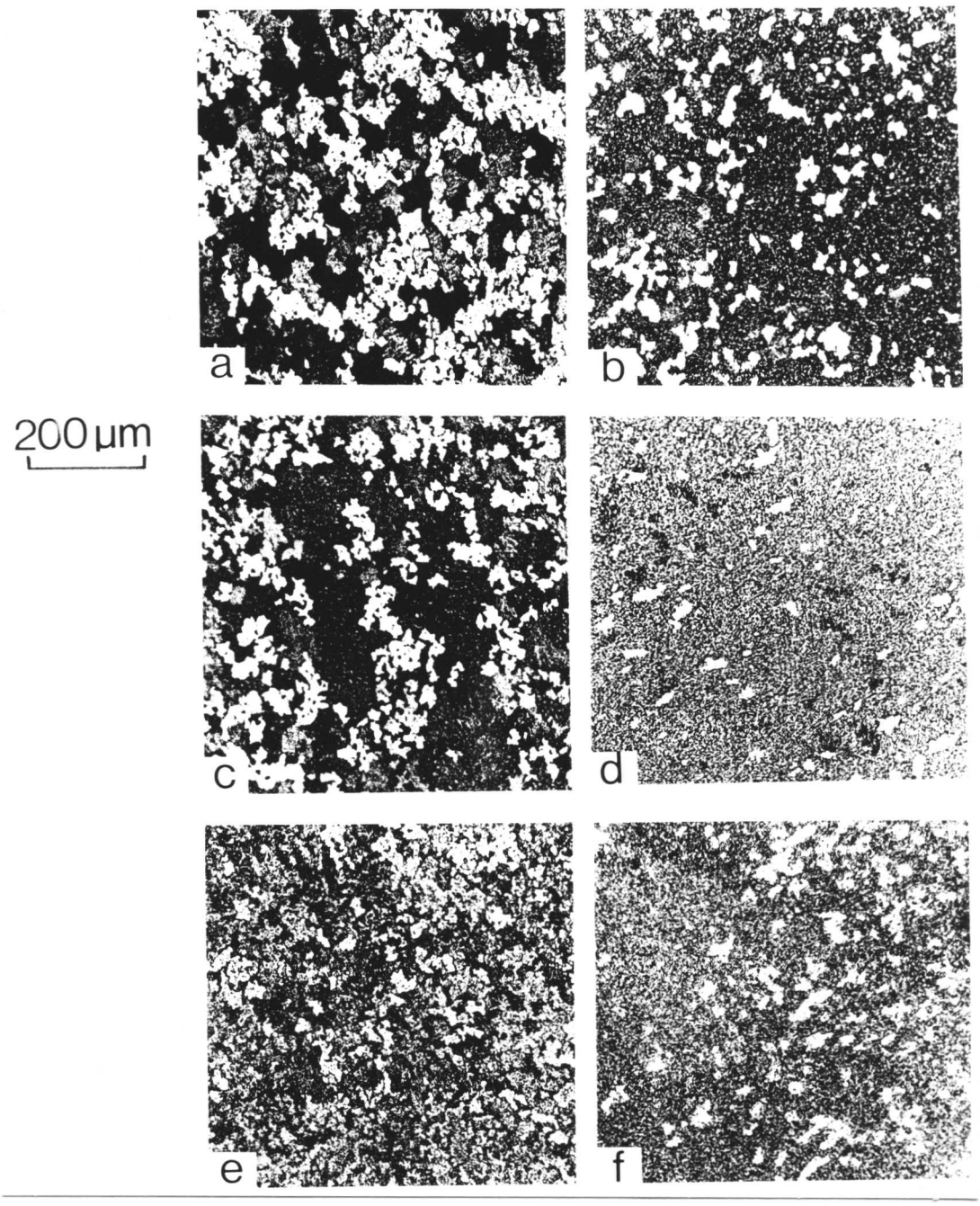

Figure 6.15. Micrographs recorded after zone annealing specimens prepared normal to the rolling direction, at T_p = 1180°C with specimen travel speeds,

a,b. 1.4 mm/min c,d. 3.2 mm/min e,f. 5.0 mm/min

Each pair of micrographs reveals the microstructure from two different parts of specimen, for example, pair a & b represents the enter part (part of specimen first passed through R. F. coil) and the middle part of specimen from where the peak temperature was recorded.

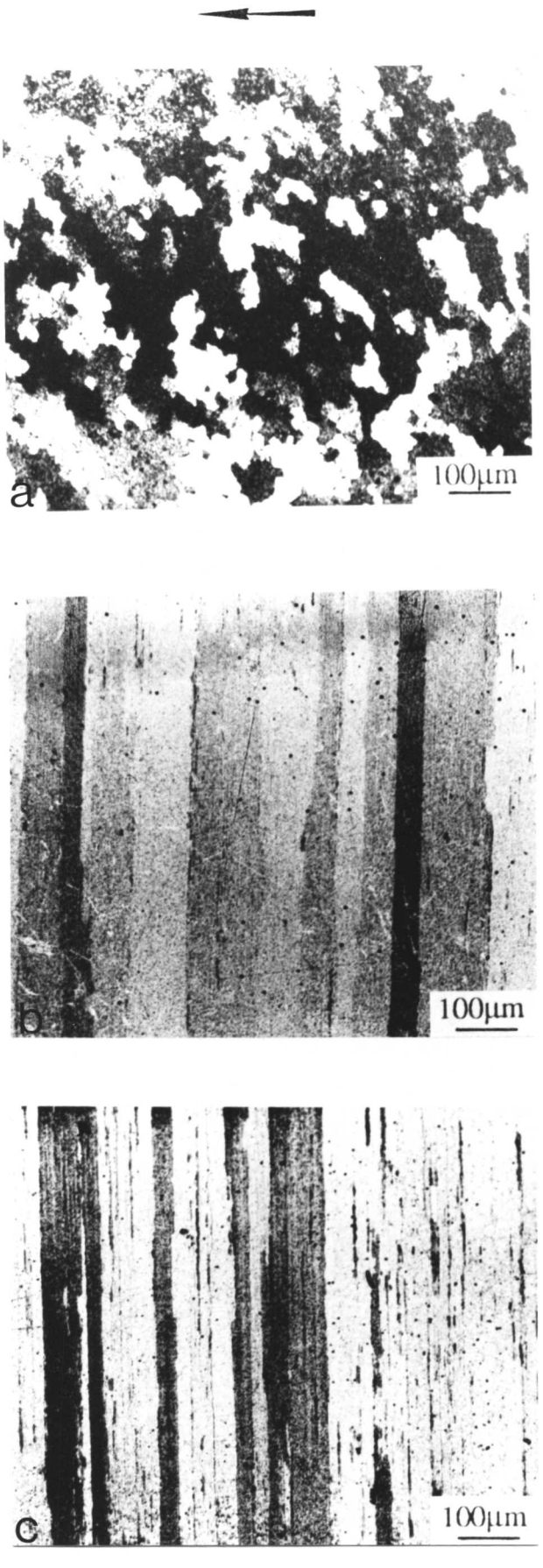

Figure 6.16. Optical micrographs recorded after zone annealing at T_p = 1280°C. Specimens prepared perpendicular to the rolling direction with specimen travel speeds. The arrow indicates the direction of zone annealing.

a. 1.4 mm/min

b. 3.2 mm/min

c. 5.0 mm/min

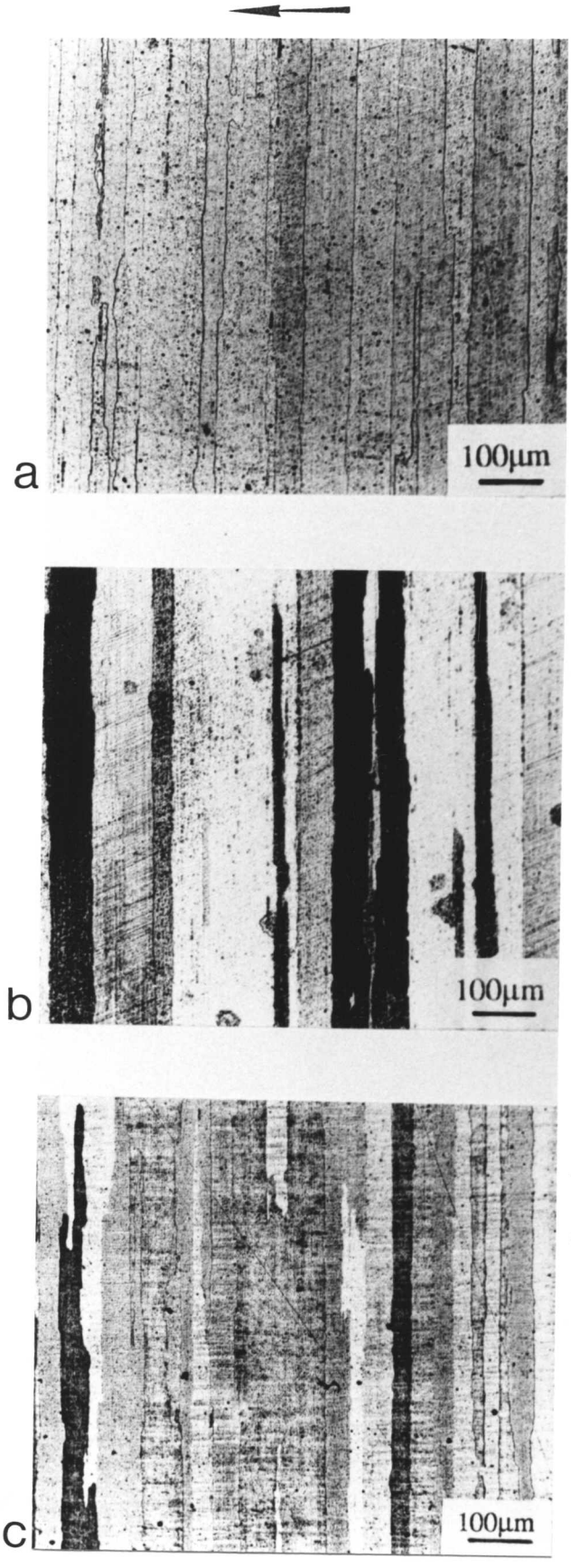

Figure 6.17. Optical micrographs recorded after zone annealing at T_p = 1380°C. Specimens prepared perpendicular to the rolling direction with specimen travel speed. The arrow indicates the direction of zone annealing.

a. 1.4 mm/min

b. 3.2 mm/min

c. 5.0 mm/min

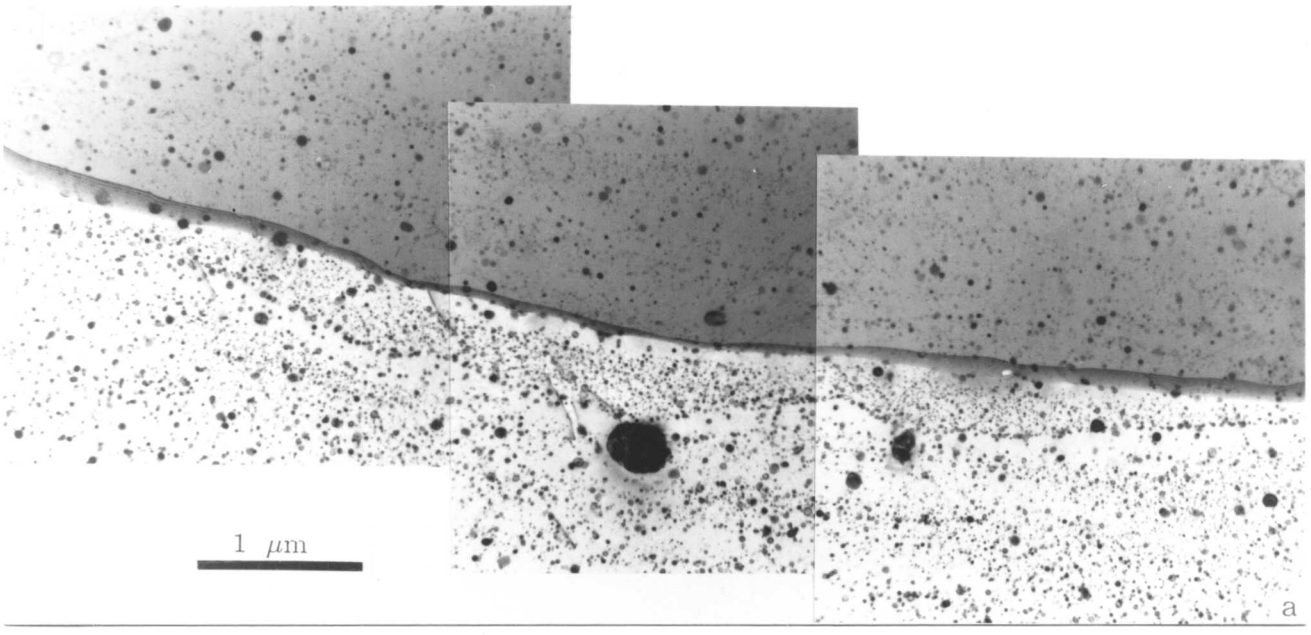

Figure 6.18. Transmission electron micrograph recorded from the thin foil prepared from specimen zone annealed at T_p = 1280°C with specimen travel speed of 3.2 mm/min. It is obvious from the micrograph that the hot rolling has a major contribution in the directional recrystallisation of Incoloy MA956, in a way that it aligns the particles along the working direction, which gives the grains an immense boost to recrystallise in unidirection during heat treatment.

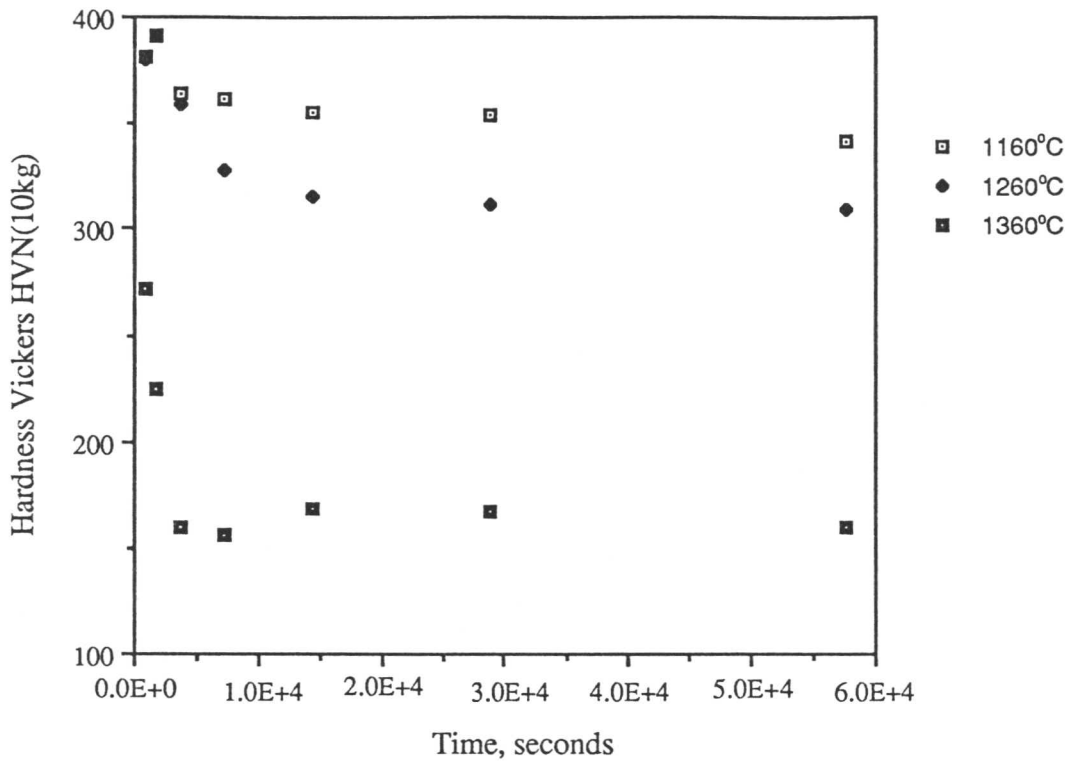

Figure 6.19. Graph showing variation in hardness versus time, after isothermal annealing at temperatures in the range 1160 to 1360°C.

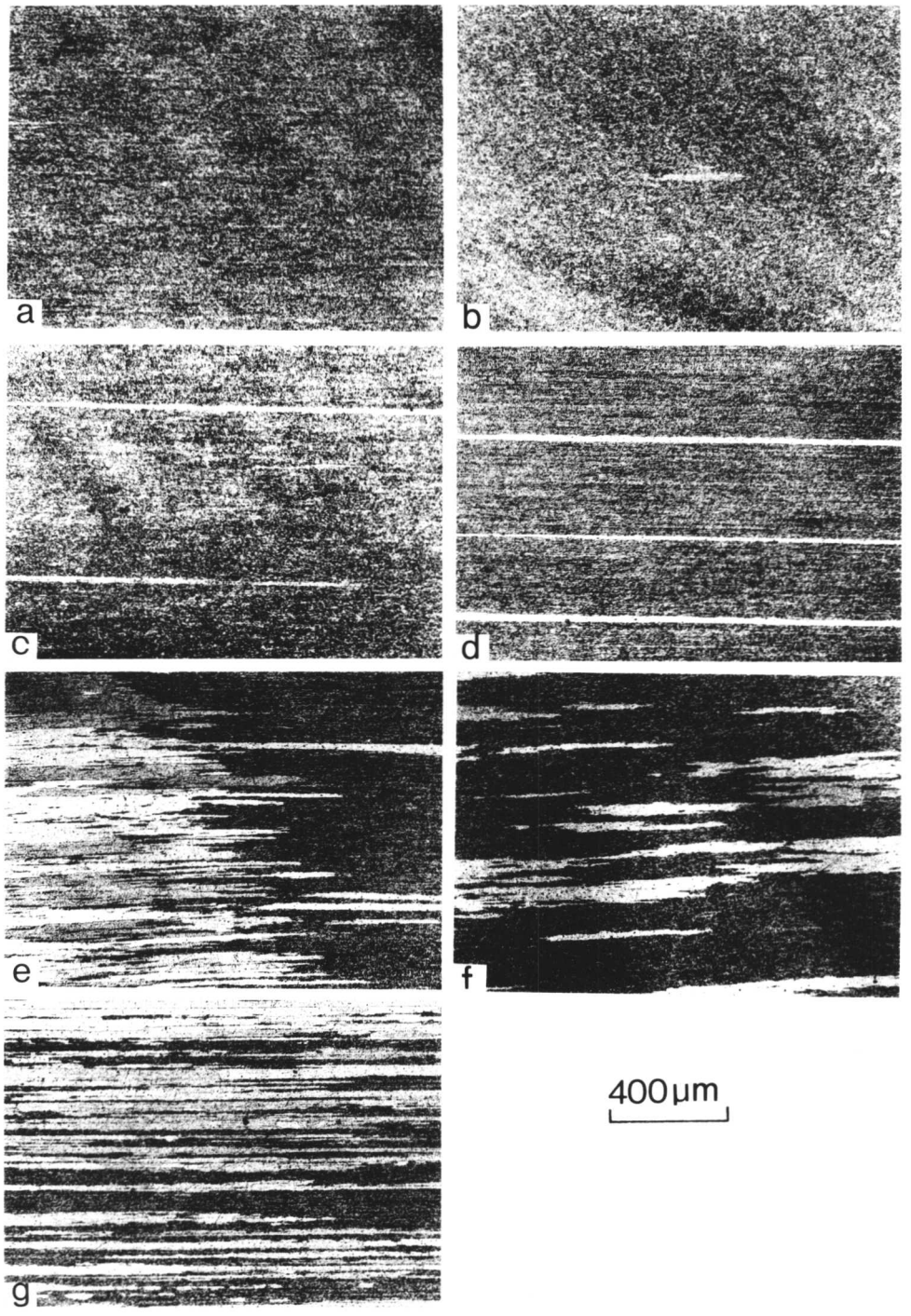

Figure 6.20. Showing the microstructure recorded after isothermal annealing specimens at 1160°C for:

a. 900 seconds
b. 1800 seconds
c. 3600 seconds
d. 7200 seconds
e. 14400 seconds
f. 28800 seconds
g. 57600 seconds

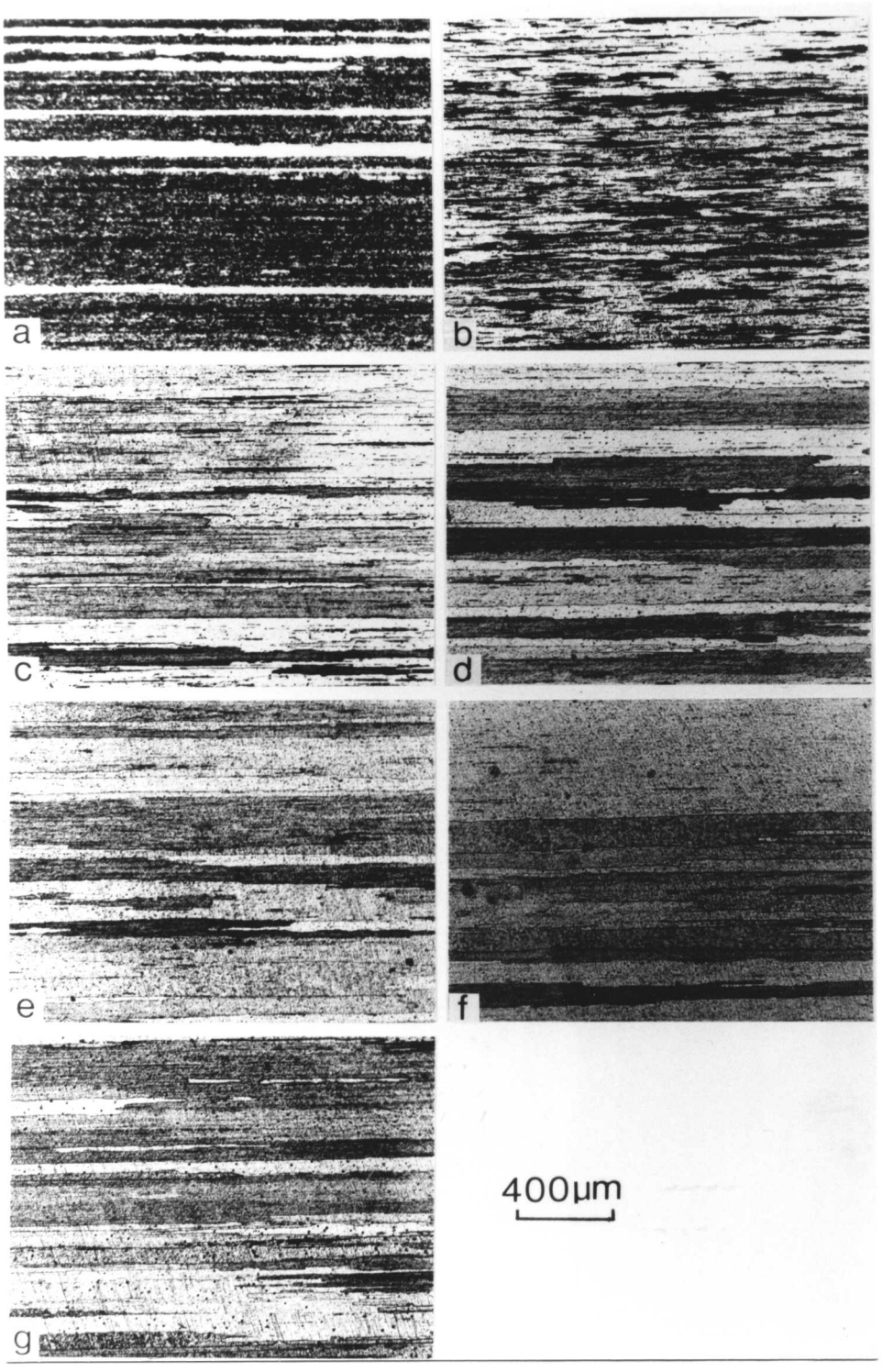

Figure 6.21. Showing the microstructure recorded after isothermal annealing at 1260°C for:

a. 900 seconds
b. 1800 seconds
c. 3600 seconds
d. 7200 seconds
e. 14400 seconds
f. 28800 seconds
g. 57600 seconds

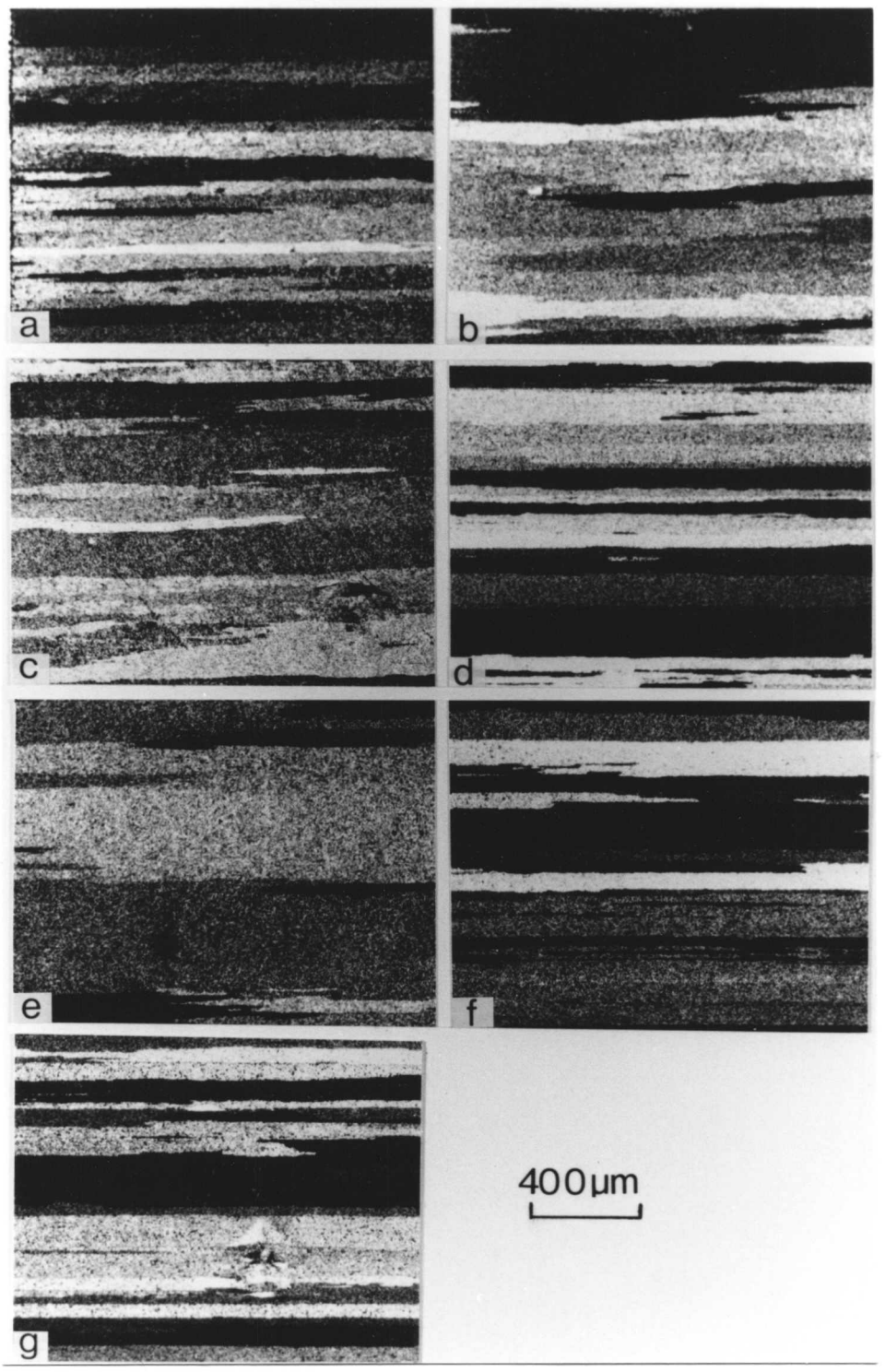

Figure 6.22. Showing the microstructure recorded after isothermal annealing specimens at 1360°C for:

a. 900 seconds
b. 1800 seconds
c. 3600 seconds
d. 7200 seconds
e. 14400 seconds
f. 28800 seconds
g. 57600 seconds.

CHAPTER SEVEN

Zone Annealing and Isothermal Annealing Experiments on Oxide Dispersion Strengthened Ferritic Steel Incoloy MA957

7.1 Introduction

It is now well-established that the incorporation of fine oxide dispersions in oxidation resistant metallic matrices can provide alloys with good high temperature strength. In addition, carefully controlled processing can induce the formation of very large elongated grains, which contribute significantly to creep resistance. Although considerable research has been done on dispersion strengthened nickel base alloys, comparatively few data are available on similar ferritic materials.

The results obtained from zone annealing and isothermal annealing experiments on experimental alloy MA957, are discussed in the present chapter.

The alloy is ferritic and is one of the more recently developed metals, which is dispersion strengthened with Y_2O_3. It is produced from powder by mechanical alloying, and its nominal chemical composition is listed in Table 7.1.

Table 7.1. Chemical composition of Incoloy alloy MA957.

Chemical composition (wt%)						
C	Cr	Al	Ti	O	Y_2O_3	Balance
0.01	14.29	1.01	0.04	0.21	0.27	Fe

7.2 Material

The alloy was supplied in the "hot-rolled" condition in the form of 1000 mm long bar of 9.5 mm diameter. Hot rolling was carried out at 1000°C with a reduction from 54 mm diameter to 9.5 mm diameter (an 82% reduction in area) being achieved in one pass.

Specimens were cut in rectangular shape with the final dimensions of 2.5 x 4 x 20 mm, the length being along the rolling direction. They were then zone annealed at three different peak

temperatures ranging from 1150 to 1350°C, using eight constant specimen travel speeds (0.2, 0.4, 0.8, 1.4, 3.2, 5.0, 7.7 and 10.0 mm/min). The hardness tests were performed using Vickers hardness testing machine. A load of 10kg was applied for each indentation.

7.3 Results and Discussion

Transmission electron micrographs of alloy MA957, taken using thin foils prepared from transverse and longitudinal sections of the bar in the as-received condition (figure 7.1a), revealed a slightly anisotropic grain structure in the transverse section of the bar but, highly elongated grains for the longitudinal section (figure 7.1). The microstructure was found to be consistent with a cold-deformed state, with an obviously high density of dislocations. The initial hardness measured in the as-received condition was found to be 410 HVN (10kg), again consistent with a cold-deformed microstructure; fully annealed iron can have a hardness of less than 200 HVN(10kg).

Optical microscopy of zone annealed specimens (T_p = 1150°C, 0.8 to 5.0 mm/min), figure 7.2, revealed no significant change in microstructure, and these observations were reflected in the high hardness values (Table 7.2a).

For the higher peak temperature of 1250°C, figure 7.3 shows that as the specimen travel speed increases the volume fraction of recrystallisation decreases until eventually, the deformed microstructure remains apparently unchanged. The material clearly shows a tendency to directionally recrystallise at T_p = 1250°C and the results are consistent with the corresponding hardness data. The hardness was noted to decrease with an increase in travel speed (Table 7.2b). A drastic difference in hardness was recorded between the recrystallised and unrecrystallised regions of the sample. An example of this is the sample zone annealed at T_p= 1250°C and 3.2 mm/min (see figure 7.3e). The hardness measurements for the recrystallised and unrecrystallised regions turned out as 181 and 357 HVN(10kg) respectively. This indicates some recovery in the apparently unrecrystallised regions.

Figure 7.4 shows a transmission electron micrograph which was taken using a thin foil prepared from the longitudinal section of the specimen zone annealed at T_p = 1250°C and a specimen travel speed of 5.0 mm/min. The microstructure observed confirms the unrecrystallised, deformed state of samples zone annealed at the faster specimen travel speeds.

Figure 7.5, shows the microstructure observed after zone annealing samples at T_p = 1350°C. It can be seen that the specimens are fully directionally recrystallised. At slower specimen travel

speeds (0.8 & 1.4 mm/min.), a columnar grain structure was observed, which had the appearance of a cast ingot, but as the specimen travel speed increased to 5.0 mm/min, relatively small but directionally recrystallised grains were observed.

The ingot type grain structure (figure 7.5a & b), was thought to be due to dominance of grains growing from the surface of the sample since the R. F. technique preferentially heats that region and the remainder of the sample increases in temperature by induction. To minimize this effect, zone annealing experiments were performed on the samples pre-annealed at 550°C for 90 hours and for 10 days. The aim was to reduce grain growth rate and thereby cut down the tendency for the favoured surface grains to dominate the microstructure. The reduction in stored energy could be measured as a decrease in hardness. The hardness for MA957 in the as-received condition, after pre-annealing at 550°C for 90 hours and 10 days was measured to be 410, 378 and 376 HVN(10kg) respectively.

Some specimens were zone annealed after pre-annealing, at peak temperatures ranging from 1150 to 1350°C. The results are illustrated in figure 7.2 which shows that for T_p below 1200°C, does not significantly influence the optical microstructure and the hardness also remains as high as it was measured from the samples zone annealed without pre-annealing (Table 7.2a).

If it is assumed that pre-annealing reduces the stored energy, then it may be concluded that a reduction in stored energy retards recrystallisation. Examination of the pre-annealed samples zone annealed at T_p = 1250°C reveals (figures 7.6, 7.7) that at a specimen travel speed of 0.2 mm/min, only partial directional recrystallisation occurs, whereas in the absence of pre-annealing, the samples are fully recrystallised (figure 7.3a). The hardness results (Table 7.2b) from those samples are also found to be in good qualitative agreement with the microstructural observations.

The micrographs shown in figures 7.8 and 7.9, were taken after zone annealing those specimens which were pre-annealed at 550°C for 90 hours and 10 days respectively. It can be seen that at the relatively high peak temperatures the microstructure obtained is not altered significantly by pre-annealing although in some cases, the fine grain structures obtained during zone annealing are replaced by more elongated grains (e.g. figures 7.5c with 7.8c and 7.9c).

An examination of thin foils prepared from longitudinal section of directionally recrystallised sample, revealed a tendency for particle alignment along the working direction (figure 7.10), although the tendency for alignment appeared less than in alloy MA956 (figure 6.8 of chapter six). This could be due to relatively smaller addition of Y_2O_3 particles (0.27 wt%) (Table 7.1), compared

with MA956 which contains 0.52 wt% Y_2O_3 particles.

There is an obvious tendency for the grain boundary to be pinned by the particles, although again, the pinning is clearly inadequate to completely stop recrystallisation. However, the effect of the oxide particles was evident in the observations of small regions of unrecrystallised material pinned and left behind as the remainder of the recrystallisation front advanced relatively rapidly (figure 7.13).

The data for T_p = 1250°C listed in Table 7.2b, give an indication of the grain boundary advancement rate, since there is a transition from a fully directionally recrystallised microstructure to one which contains some recrystallised grains in a partially recrystallised sample. There is clearly no difficulty in nucleating new grains, but due to faster specimen travel speed these grains are not capable to keep up with motion of the sample, the specimen travel speed gives an upper limit to the grain boundary velocity.

The concept of "kinetic strength" D and "effective temperature" T_E, discussed in an earlier chapter and mathematically expressed in equations 6.4 and 6.6 respectively, have been applied to measure the activation energy Q, from the experimental data (figure 7.14i) obtained after zone annealing samples MA957 at peak temperatures ranging from 1150 to 1350°C.

As described in the previous chapter, the effective temperature (T_E) allows an experimental evaluation of the activation energy Q, by performing zone annealing experiments at two different peak temperatures and a range of specimen travel speeds. The velocities (0.4 mm/min and 7.7 mm/min) at peak temperatures (T_p = 1250 and 1350°C respectively), where transitions from partial directional to fully directional recrystallisation were identified, and have been used to measure the activation energy.

The measured value of Q for alloy MA957 was found to be 654257 J mol^{-1}, which is much larger than that of alloy MA956 (402791 J mol^{-1}). This significant difference in the measured activation energies of two identically processed alloys (MA957 and MA956) may be due to the amount of deformation applied to each alloy 82% and 54% reduction respectively. Although MA957 has a lower oxide content, the tendency for particle alignment is smaller, so that grain boundary mobility along the annealing direction may be more effectively impeded.

By integrating the data measured during operation at the peak temperatures ranging from 1150 to 1350°C with a variety of specimen travel speeds, graphs have been plotted for exp (-Q / RT) versus time (figure 7.15).

The area under each curve (D) was calculated from the graphs shown in figure 7.14, with each curve based on the measured value of Q (654257 J mol^{-1}). The calculated value of D was then used to plot the graphs for the integral D (seconds) versus velocity (mm/min), as shown in figure 7.16, which shows that the transition from directional recrystallisation to partial directional recrystallisation comes at approximately same value of kinetic strength irrespective of temperature. The results are consistent with the theory except for the conditions where no recrystallisation was observed.

The following notation is used to indicate the microstructure and processing in the tables used to summarise the experimental data:

Symbols	Terms
D	As-deformed
DX	Directionally recrystallised
HV	Vickers hardness
Pre Ald	Pre-annealed at 550°C for 90 hours and 10 days
PDX	Partial directionally recrystallised
Pl: RD	Parallel to the rolling direction
T_p	Peak temperature
PX	partially recrystallised
X	Recrystallised with an equiaxed grain structure.

Table 7.2a. Microstructure and Vickers hardness data obtained for Inconel alloy MA957, after zone-annealir condition and after annealing at 550 ^{0}C for 90 hrs and 10 days. Hardnesses measured in the as-received cond 410, 378 and 376 HVN(10kg) respectively.

T_P ^{o}C	Specimen	Specimen Travel Speed mm/min				Hardness Vickers HVN(10kg)				Mean H
	Condition	0.8	1.4	3.2	5.0	0.8	1.4	3.2	5.0	0.8
1150	Pl: RD as-received condition	D	D	D	D	366 373 380 373 376	366 370 373 376 373	387 387 394 390 387	366 373 373 376 366	374
1150	Pre-Ald at 550^{o}C for 90 hrs	D	D	D	D	360 363 370 373 370	354 366 376 376 366	363 366 363 370 360	357 360 360 370 370	367
1150	Pre-Ald at 550^{o}C for 10 days	D	D	D	D	363 366 366 363 366	357 357 360 360 357	354 345 363 360 354	366 370 370 366 366	365

Table 7.2b. Microstructure and Vickers hardness data obtained for Inconel alloy MA957, after zone-anne condition and after annealing at 550 ^{0}C for 90 hrs and 10 days. Hardnesses measured in the as-received c 410, 378 and 376 HVN(10kg) respectively.

T_P °C	Specimen	Specimen Travel Speed mm/min						Hardness Vickers HVN(10kg)						Mea
	Condition	0.2	0.4	0.8	1.4	3.2	5.0	0.2	0.4	0.8	1.4	3.2	5.0	0.2
1250	Pl: RD as-received condition	DX	PDX	PDX	PDX	PX	D	168	178	172	176	317	312	178
								177	192	170	325	325	314	
								205	315	306	354	357	317	
								171	312	306	333	327	314	
								171	309	306	330	181	312	
1250	Pre-Ald at 550°C for 90 hrs	PDX	PDX	PDX	D	D	D	167	309	312	299	294	306	227
								170	312	319	315	304	312	
								205	306	330	319	315	317	
								294	309	325	312	309	315	
								299	254	322	315	309	312	
1250	Pre-Ald at 550°C for 10 days	DX	PDX	D	D	D	D	165	285	294	319	327	322	217
								168	306	304	333	325	336	
								309	317	309	345	327	348	
								272	315	306	330	322	322	
								170	309	306	327	319	315	

Table 7.2c. Microstructure and Vickers hardness data obtained for Inconel alloy MA957, after zone-annealing condition and after annealing at 550 ^{0}C for 90 hrs and 10 days. Hardnesses measured in the as-received condi 410, 378 and 376 HVN(10kg) respectively.

T_P °C	Specimen	Specimen Travel Speed mm/min						Hardness Vickers HVN(10kg)						Mea
	Condition	0.8	1.4	3.2	5.0	7.7	10.0	0.8	1.4	3.2	5.0	7.7	10.0	0.8
1350	PI: RD as-received condition	DX	DX	DX	DX	PDX	PX	159	161	160	166	170	260	161
								163	165	166	170	197	302	
								157	165	167	171	235	304	
								168	160	170	167	212	299	
								160	170	170	160	193	302	
1350	Pre-Ald at 550°C for 90 hrs	DX	DX	DX	DX	PDX	PX	154	156	162	173	167	272	158
								157	154	175	172	170	294	
								157	152	167	166	289	304	
								159	165	182	177	173	287	
								161	160	167	166	167	166	
1350	Pre-Ald at 550°C for 10 days	DX	DX	DX	DX	PDX	PX	158	166	167	168	160	161	165
								177	192	169	159	164	167	
								165	177	197	170	162	181	
								166	177	164	167	180	162	
								159	169	170	164	169	166	

7.4 Isothermal Annealing of ODS Alloy MA957

Isothermal annealing experiments were also performed on MA957, using conventional resistance furnaces set at temperatures ranging from 1160 to 1360°C. The annealing time was initially 900 seconds, the time period being doubled for each successive heat treatment, to a maximum of 57600 seconds. The hardnesses (HVN) data for the annealed samples are listed in Table 7.3 and illustrated in figure 7.17.

Figure 7.18 shows the microstructure after each successive annealing treatment at 1160°C. Even for the maximum annealing time (57600 seconds), the microstructure does not seem to have altered at all, consistent with the corresponding high hardness values (Table 7.3).

As the isothermal annealing temperature was raised to 1260°C the material was found to recrystallise but the longer incubation time was observed compared with zone annealing at almost same peak temperature (T_p = 1250°C). Figure 7.19 and 7.3 illustrate such an observation. The reason why the specimens tend to recrystallise in shorter period of time during zone annealing may be because regions outside the hot zone do not undergo recovery as the recrystallisation front progresses. During isothermal annealing on the other hand, all regions are at the annealing temperature and may undergo a larger degree of recovery prior to recrystallisation.

Even after 7200 seconds at 1260°C, it was possible to find regions of unrecrystallised microstructure, and prolonged annealing resulted in the formation of recognisable regions of recrystallised equiaxed grains. The specimens were not found to be fully recrystallised even after isothermal annealing at 1260°C for 57600 seconds. It seems that much more longer time is required to obtain fully recrystallised grain structure at 1260°C during isothermal annealing when compared with zone annealing.

At relatively higher annealing temperatures (1360°C) specimens were found to directionally recrystallise during conventional annealing treatment (figure 7.20a-d), and the hardness results (Table 7.2c) from those samples are found to be in good agreement with the microstructural observations.

Table 7.3. Hardness (HVN) data obtained after isothermal annealing of MA957 at different temperatures and for a variety of time periods.

Temperature	Annealing time in seconds						
°C	900	1800	3600	7200	14400	28800	57600
	Hardness HVN(10kg)						
1160	381	379	362	358	353	351	339
	381	394	362	360	353	353	341
	381	396	367	362	356	358	341
	381	394	365	362	356	353	341
	388	378	362	360	356	353	339
	Mean hardness values						
	382	388	364	360	355	354	340
1260	379	386	353	329	313	312	289
	379	388	360	329	315	308	319
	379	396	362	327	313	312	313
	381	394	360	329	317	315	315
	379	386	353	325	313	315	312
	Mean hardness values						
	379	384	258	328	314	312	310
1360	162	181	154	157	166	169	160
	298	286	155	157	162	168	157
	329	312	158	157	164	167	160
	291	172	169	150	169	163	165
	282	169	166	157	178	166	159
	Mean hardness values						
	272	224	160	156	168	167	160

7.5 Conclusions

It appears that alloy MA957 has tendency to directionally recrystallise upon heating in a temperature gradient. The directional recrystallisation behaviour seems to be effectively influenced by the amount of deformation applied prior to application of any heat treatment.

The oxide particles were found to be aligned by the grain boundary traces, although the tendency for alignment appeared to be less than in alloy MA956.

It was possible to approximately rationalise the behaviour of the alloy during anisothermal annealing using concept of "kinetic strength", and the effective activation energy was measured and found to be very large when compared with that of self diffusion in iron. The value of activation energy measured was also found to be larger than that for alloy MA956, perhaps because of the more isotropic dispersion of particles in MA957.

Columnar grains with an appearance of cast ingot type grain structure were sometimes observed, an effect which was thought to be due to dominance of grains growing from the surface of the sample during zone annealing. It is found possible to reduce this effect by pre-annealing at lower temperatures prior to zone annealing.

A microstructure consisted of equiaxed grains was observed after isothermal annealing at relatively lower temperature but at high temperatures the alloy exhibited directionally recrystallised grain structure. It seems that the higher amount of energy stored due to degree of deformation, boost the growth of grains along the rolling direction.

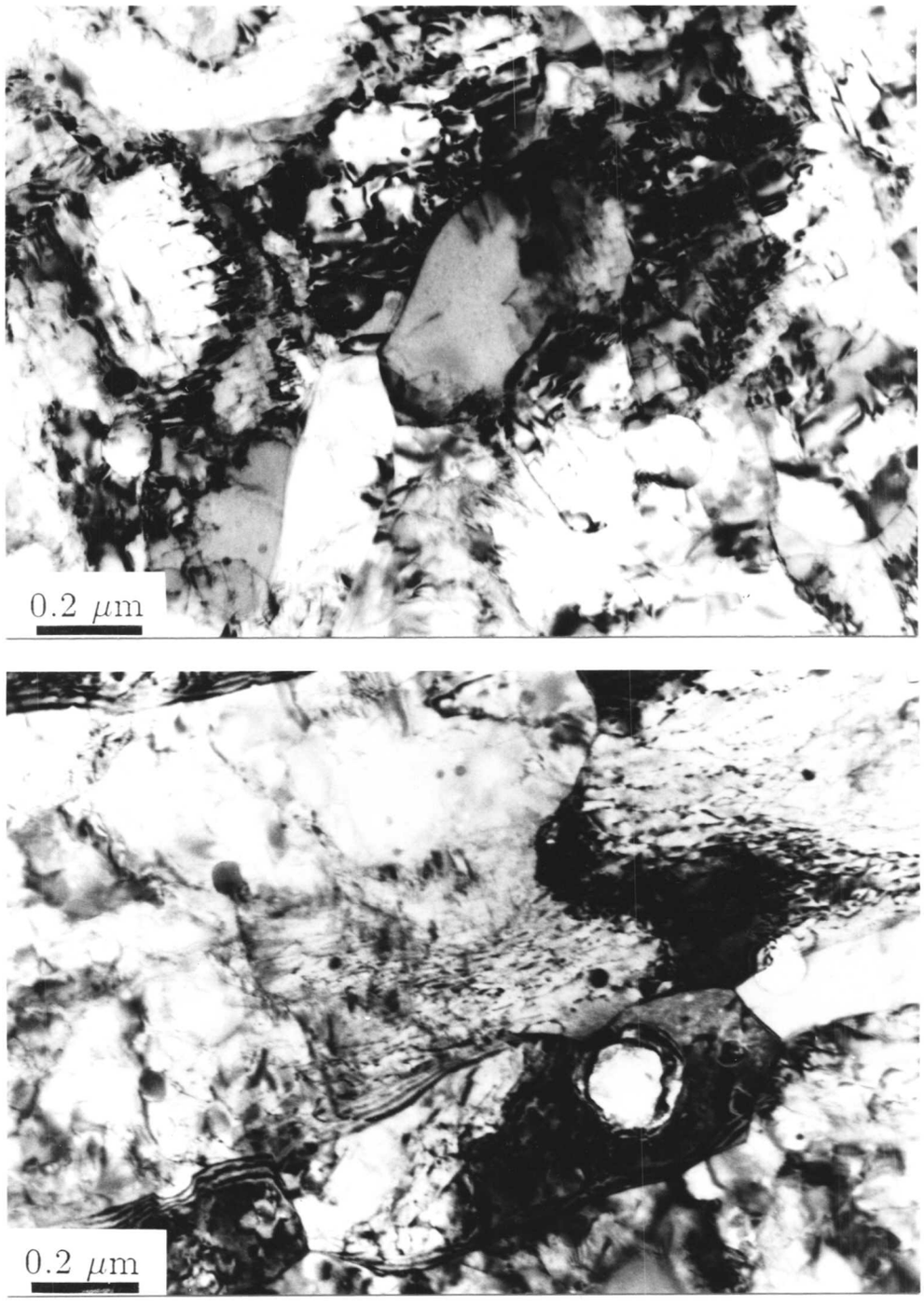

Figure 7.1. Transmission electron micrograph reveals the microstructure of alloy MA957 in the as-received condition.

a. Slightly anisotropic grain structure in a thin foil prepared from the transverse section of the hot rolled bar of MA957 in as-received condition.

b. Micrograph showing a highly elongated grain structure containing a high dislocation density in the longitudinal section of the as-received MA957 bar.

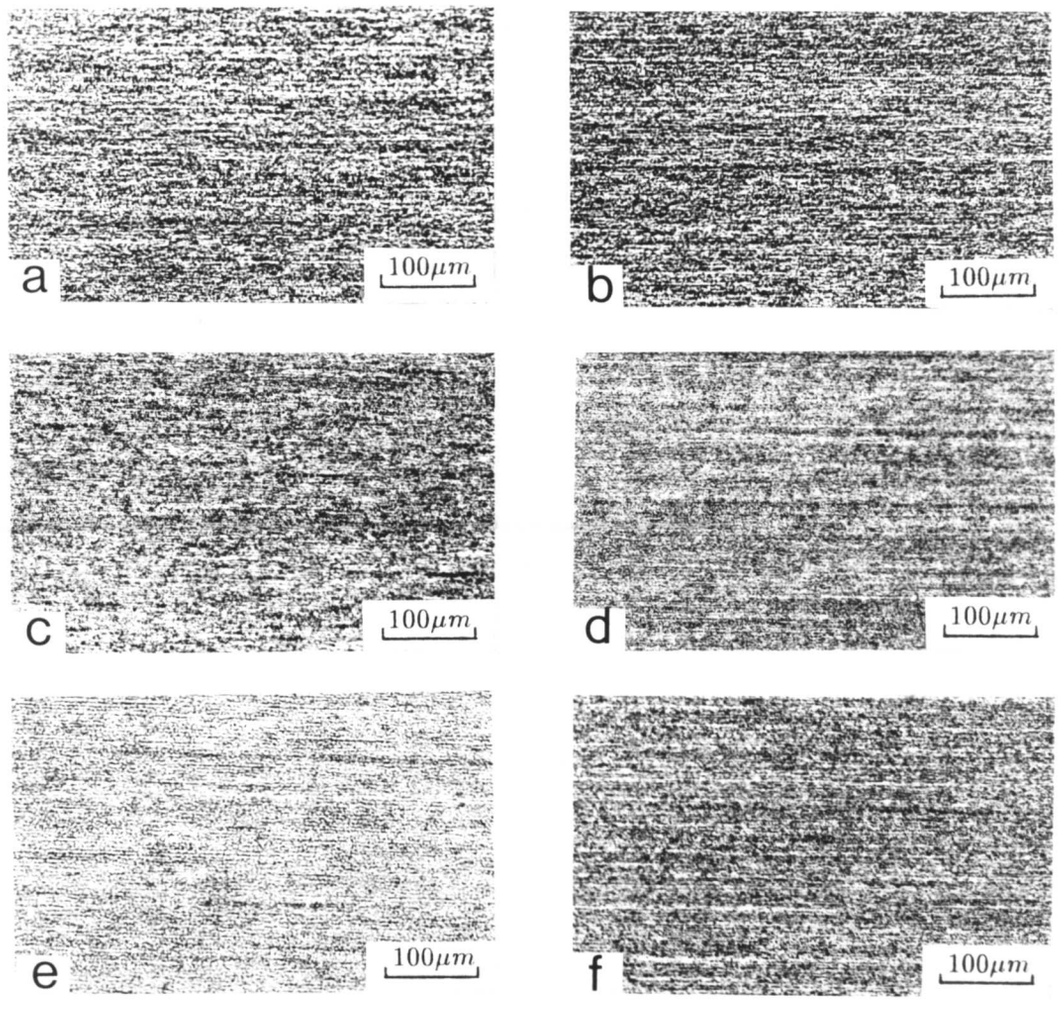

Figure 7.2. Light optical micrographs taken from the samples zone annealed at T_p = 1150°C. Micrographs a and b are from samples zone annealed in the as-received condition at specimen travel speeds of 0.8 and 5.0 mm/min respectively. Micrographs c and d are taken from the samples zone annealed after pre-annealing at 550°C for 90 hours, with specimen travel speeds of 0.8 and 5.0 mm/min respectively. Micrographs e and f are taken from the samples zone annealed after pre-annealing at 550°C for 10 days, with specimen travel speeds of 0.8 and 5.0 mm/min respectively.

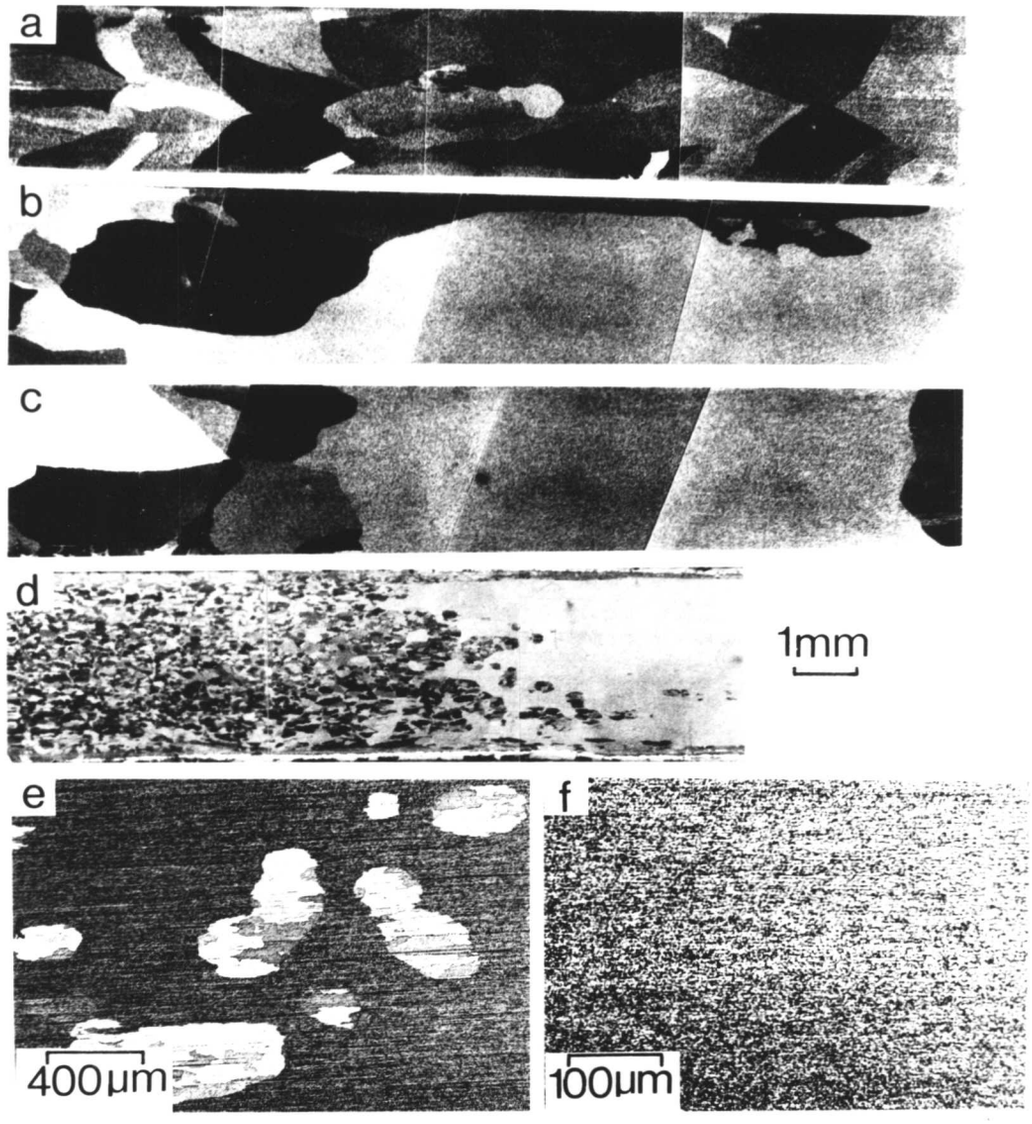

Figure 7.3 Optical micrographs showing the microstructure observed from the samples zone annealed at T_p = 1250°C, in the as-received condition at the specimen travel speeds as given below,

a. 0.2 mm/min b. 0.4 mm/min

c. 0.8 mm/min d. 1.4 mm/min

e. 3.2 mm/min f. 5.0 mm/min

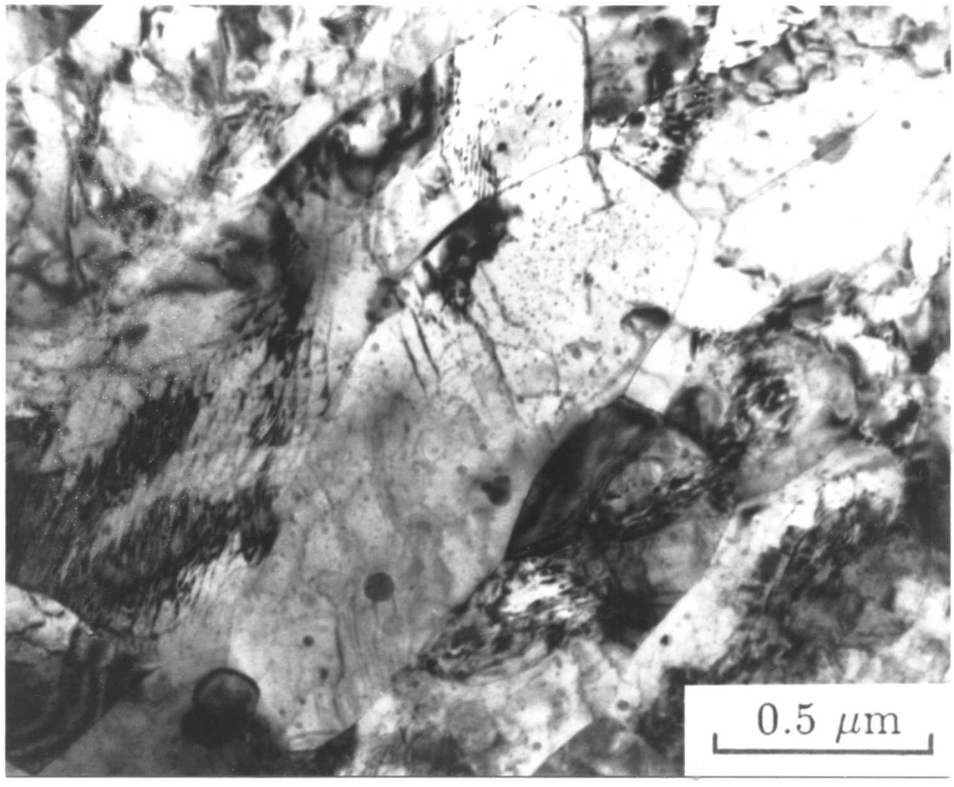

Figure 7.4. Transmission electron micrograph reveals deformed microstructure of the sample zone annealed in the as-received condition at T_p = 1250°C with a specimen travel speed of 5.0 mm/min. Micrograph taken from the longitudinal section of the sample.

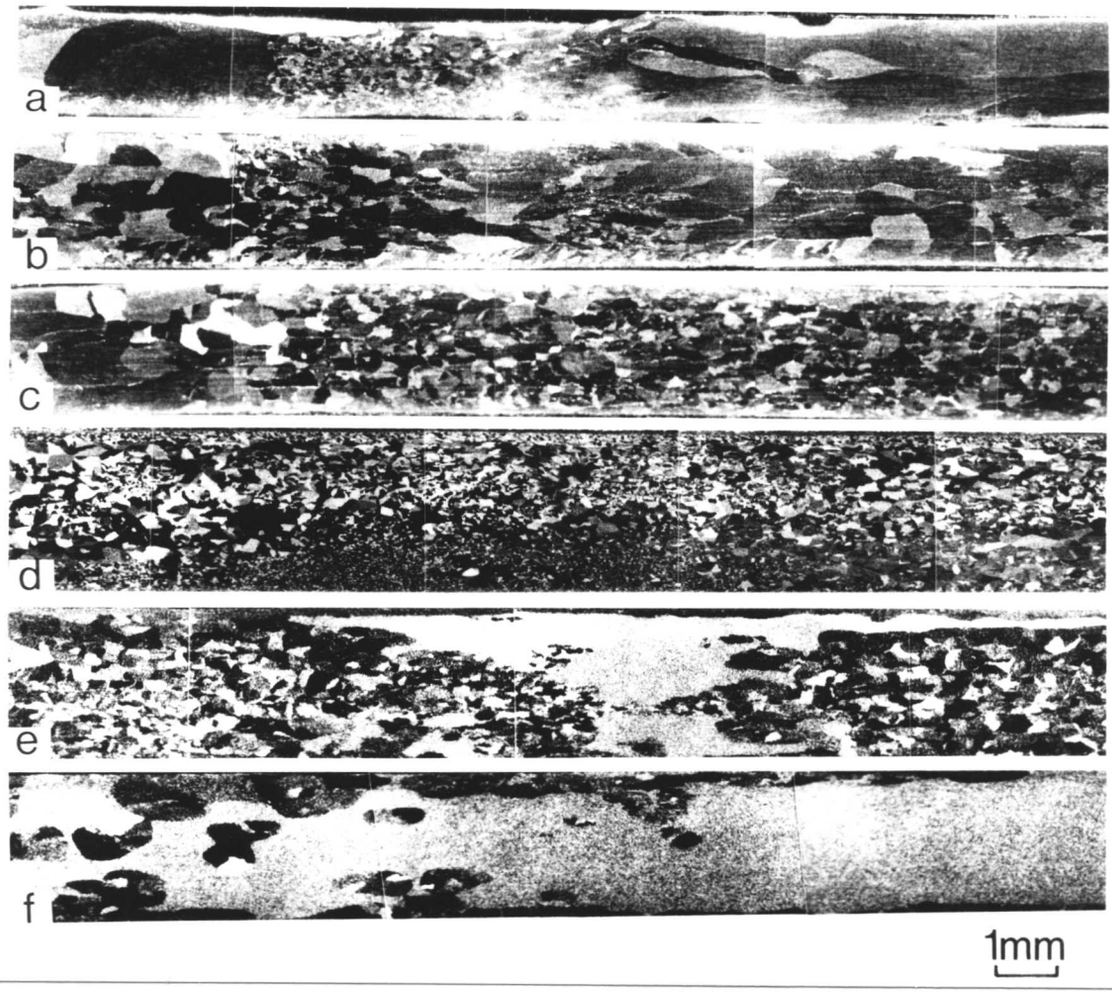

Figure 7.5. Optical micrographs showing the microstructure taken after zone annealing samples in the as-received condition at T_p = 1350°C, at the specimen travel speeds as given below:

a. 0.8 mm/min b. 1.4 mm/min

c. 3.2 mm/min d. 5.0 mm/min

e. 7.7 mm/min f. 10.0 mm/min

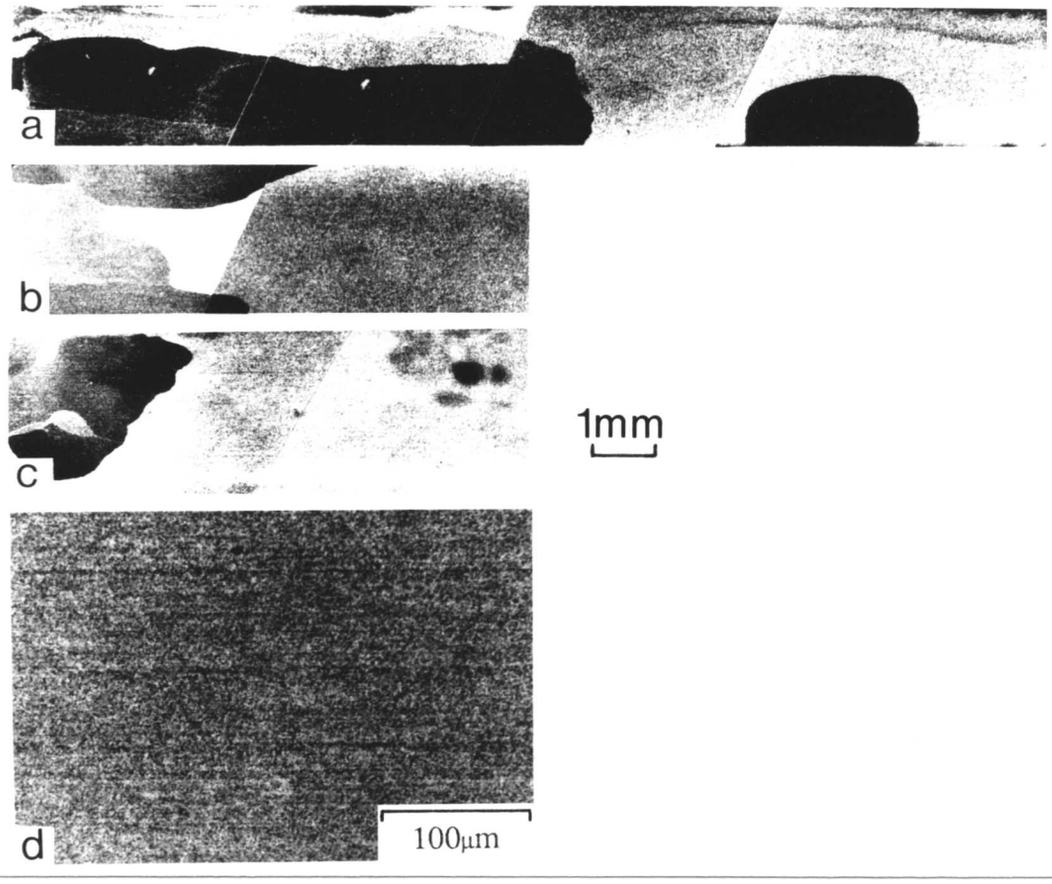

Figure 7.6. Optical micrographs taken from the samples zone annealed at T_p = 1250°C after pre-annealing at 550°C for 90 hours. The samples zone annealed with the specimen travel speeds as follows:

a. 0.2 mm/min b. 0.4 mm/min

c. 0.8 mm/min d. 1.4 mm/min

More samples have been zone annealed with the specimen travel speeds ranging up to 5.0 mm/min. Since the samples revealed as-deformed microstructure as shown for (d). So it was not felt necessary to show the micrographs recorded from those specimens.

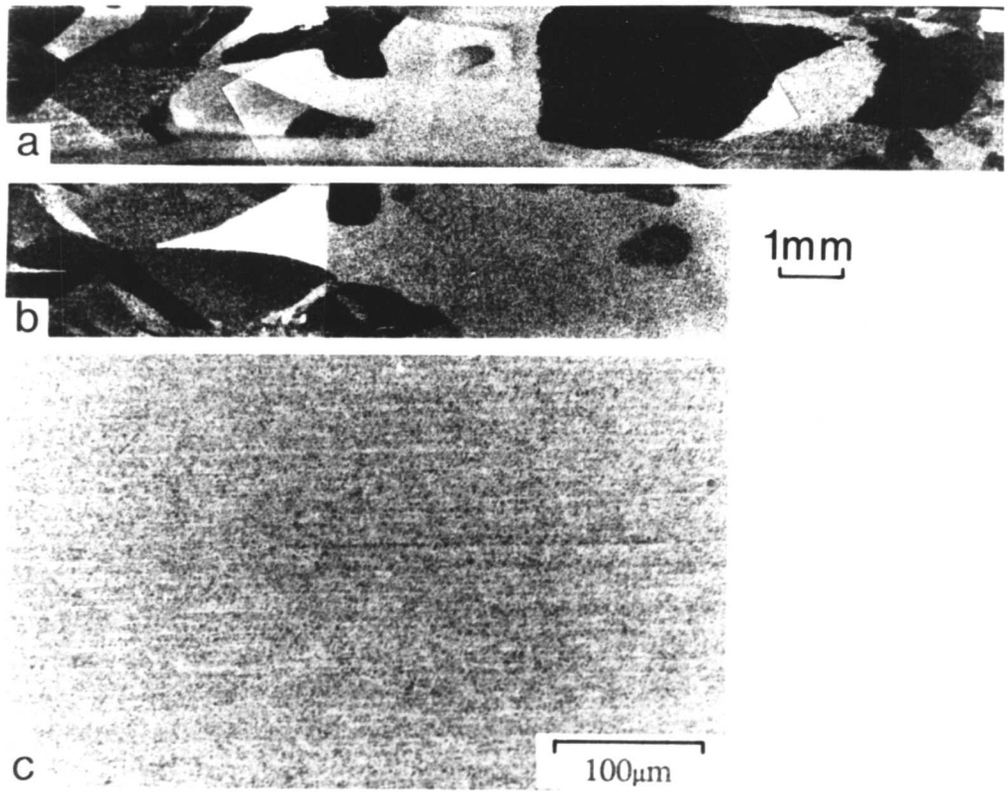

Figure 7.7. Optical micrographs taken from the samples zone annealed at T_p = 1250°C after pre-annealing at 550°C for 10 days. The specimen travel speeds are:

a. 0.2 mm/min

b. 0.4 mm/min

c. 0.8 mm/min

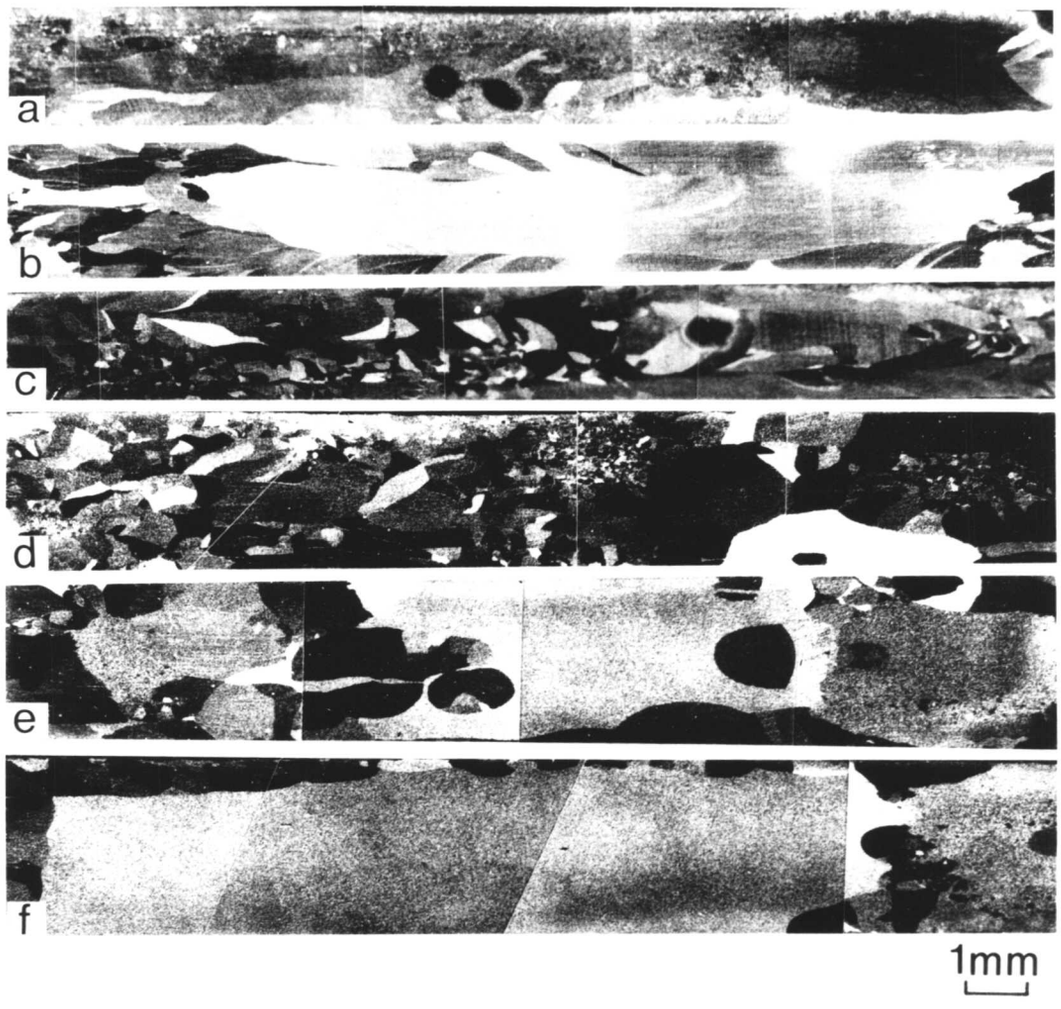

Figure 7.8. Optical micrographs taken from the samples zone annealed at T_p = 1350°C after pre-annealing at 550°C for 90 hours. The specimen travel speeds are:

a. 0.8 mm/min b. 1.4 mm/min

c. 3.2 mm/min d. 5.0 mm/min

e. 7.7 mm/min. f. 10.0 mm/min.

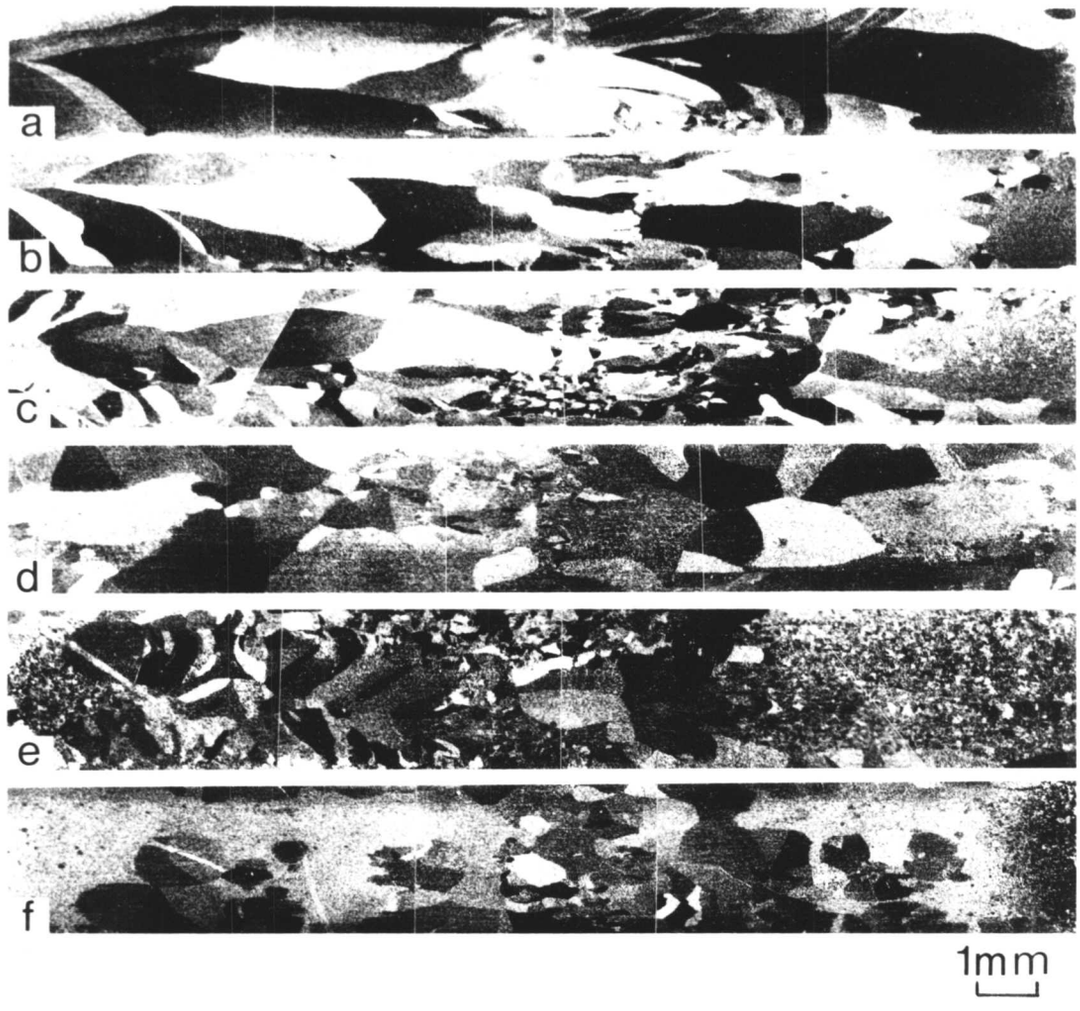

Figure 7.9. Optical micrographs taken from the samples zone annealed at T_p = 1350°C after pre-annealing at 550°C for 10 days. The specimen travel speeds are:

a. 0.8 mm/min b. 1.4 mm/min

c. 3.2 mm/min d. 5.0 mm/min

e. 7.7 mm/min f. 10.0 mm/min

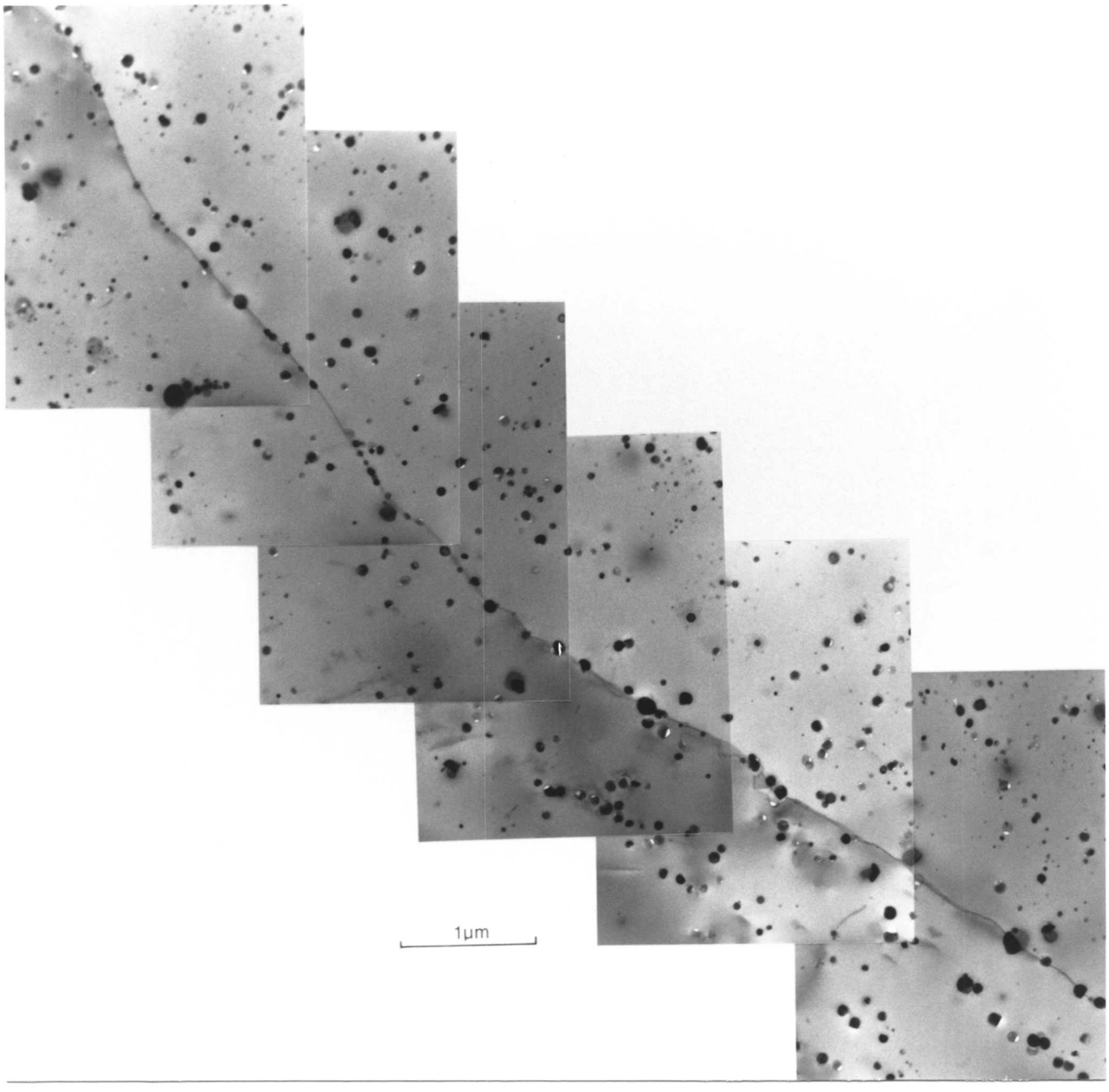

Figure 7.10. Transmission electron micrograph a thin foil, prepared from the longitudinal section of the sample zone annealed at 1250°C (0.2 mm/min).

There is clearly some indication of particle alignment along the working direction (≈ indicated by the grain boundary trace) although the extent of alignment is not as high as in alloy MA956.

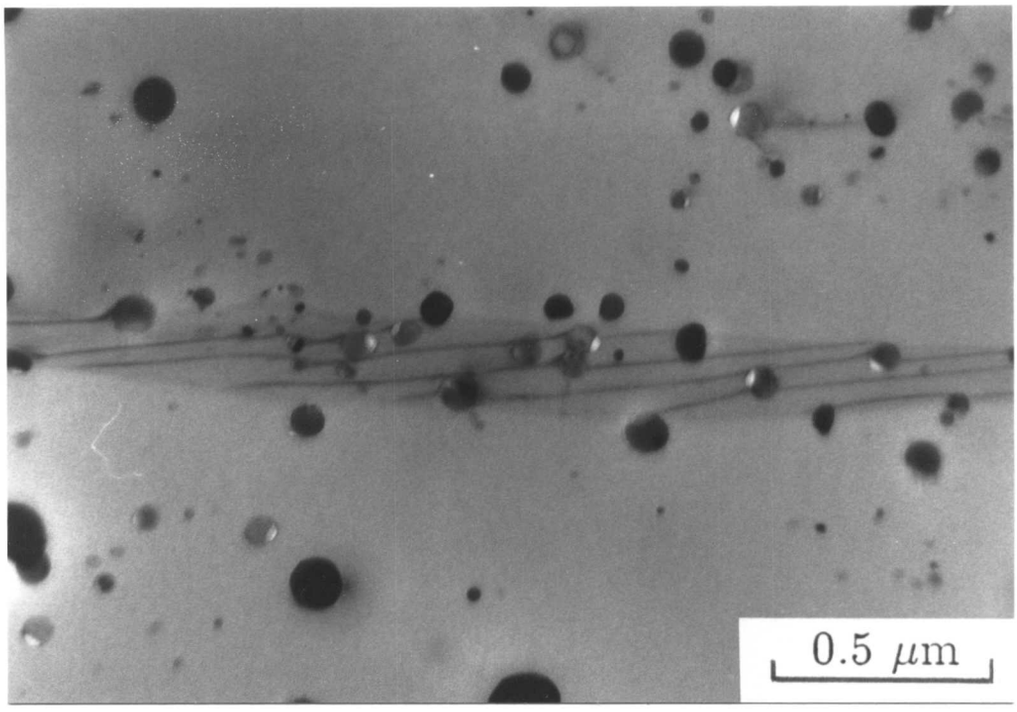

Figure 7.11. Transmission electron micrograph showing particles on the grain boundary. The micrograph was taken from a thin foil prepared from a longitudinal section of the sample zone annealed at 1250°C (0.2 mm/min).

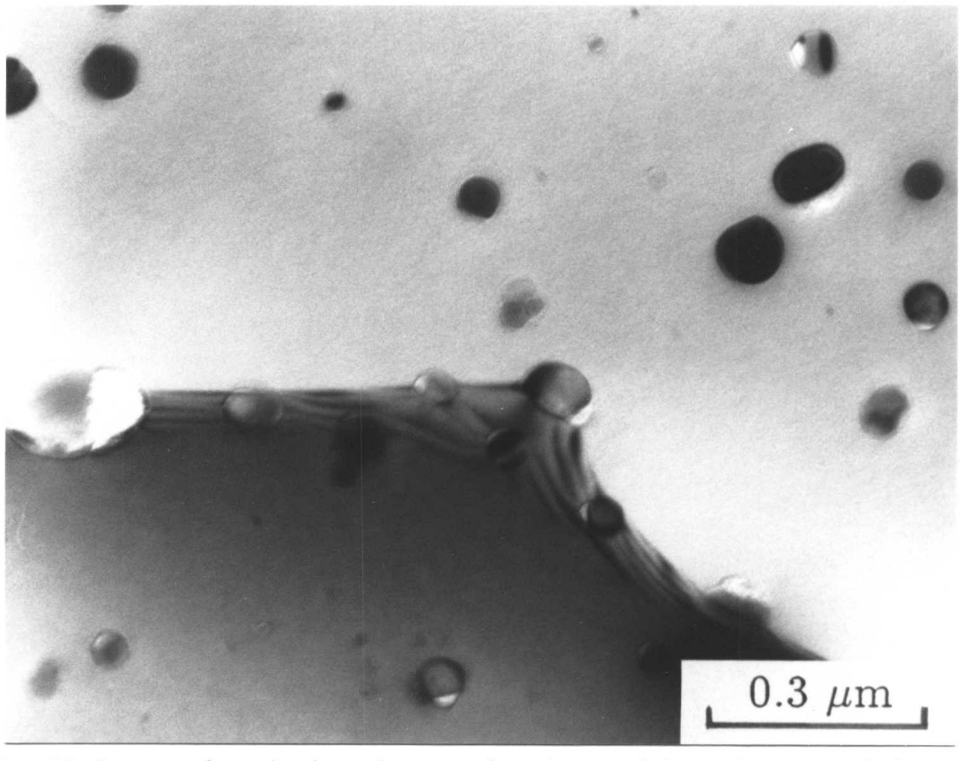

Figure 7.12. The hindrance of grain boundary motion by particles. The transmission electron micrograph was taken using a thin foil prepared from the longitudinal section of specimen zone annealed at 1250°C (0.2 mm/min).

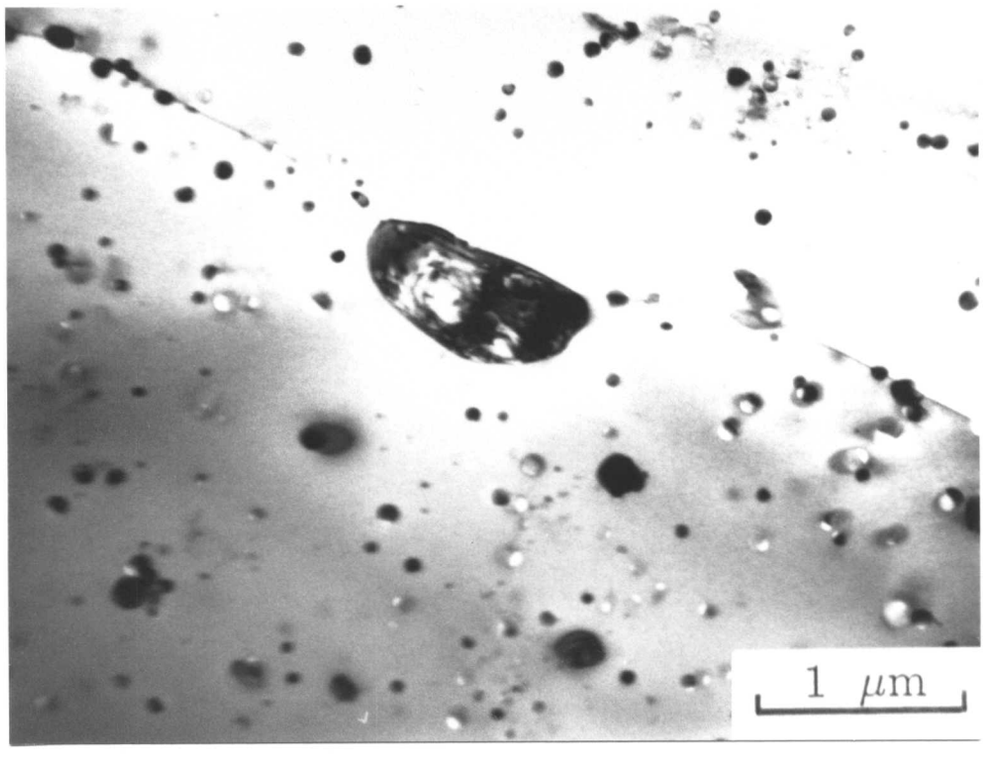

Figure 7.13. Transmission electron micrograph showing an unrecrystallised region between two fully recrystallised columnar grains of ODS alloy MA957. The micrograph is of a thin foil prepared from the longitudinal section of the sample zone annealed at 1350°C (3.2 mm/min).

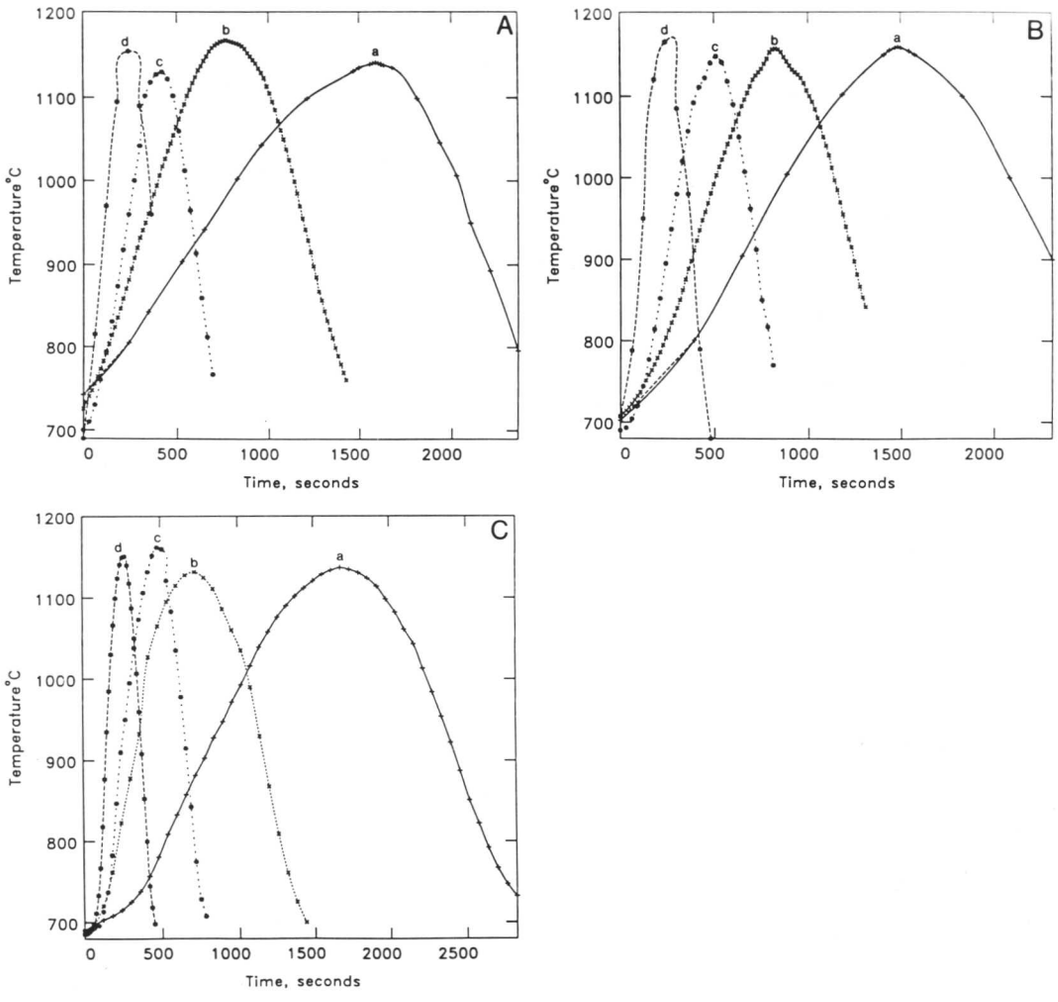

Figure 7.14(i). Temperature (°C) versus time (seconds) profiles, for samples of ODS alloy MA957, which were zone annealed (A) in the as-received condition, (B & C) after pre-annealing at 550°C for 90 hours and 10 days respectively, at T_p = 1150°C.

Figure	T_p	Profiles	Specimen travel speeds mm/min.
7.14iA.	1150°C	a - d	0.8, 1.4, 3.2 and 5.0
7.14iB.	1150°C	a - d	0.8, 1.4, 3.2 and 5.0
7.14iC.	1150°C	a - d	0.8, 1.4, 3.2 and 5.0

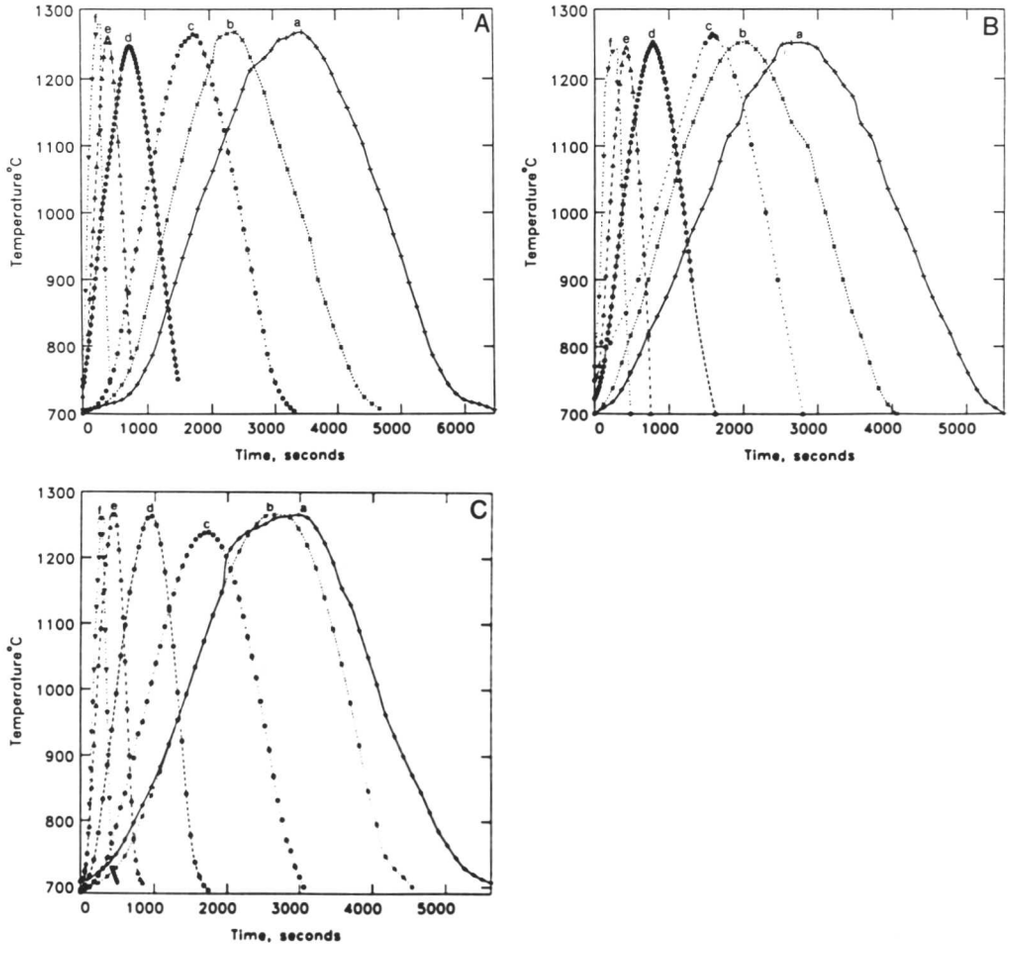

Figure 7.14(ii). Temperature (°C) versus time (seconds) profiles, for samples of ODS alloy MA957, which were zone annealed (A) in the as-received condition, (B & C) after pre-annealing at 550°C for 90 hours and 10 days respectively, at T_p = 1250°C.

Figure	T_p	Profiles	Specimen travel speeds mm/min.
7.14iiA.	1250°C	a - f	0.2, 0.4, 0.8, 1.4, 3.2 and 5.0
7.14iiB.	1250°C	a - f	0.2, 0.4, 0.8, 1.4, 3.2 and 5.0
7.14iiC.	1250°C	a - f	0.2, 0.4, 0.8, 1.4, 3.2 and 5.0

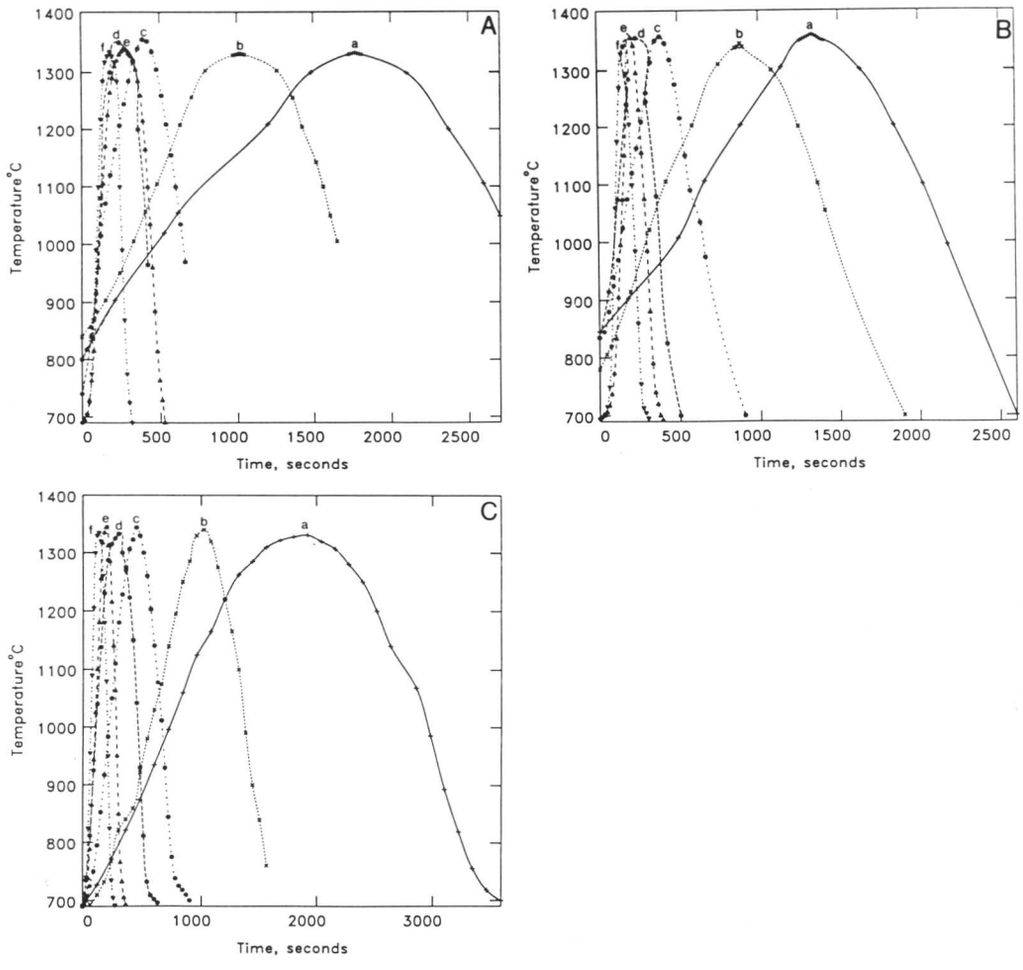

Figure 7.14(iii). Temperature (°C) versus time (seconds) profiles, for samples of ODS alloy MA957, which were zone annealed (A) in the as-received condition, (B & C) after pre-annealing at 550°C for 90 hours and 10 days respectively, at T_p = 1350°C.

Figure	T_p	Profiles	Specimen travel speeds mm/min.
7.14iiiA.	1350°C	a - f	0.8, 1.4, 3.2, 5.0, 7.7 and 10.0
7.14iiiB.	1350°C	a - f	0.8, 1.4, 3.2, 5.0, 7.7 and 10.0
7.14iiiC.	1350°C	a - f	0.8, 1.4, 3.2, 5.0, 7.7 and 10.0

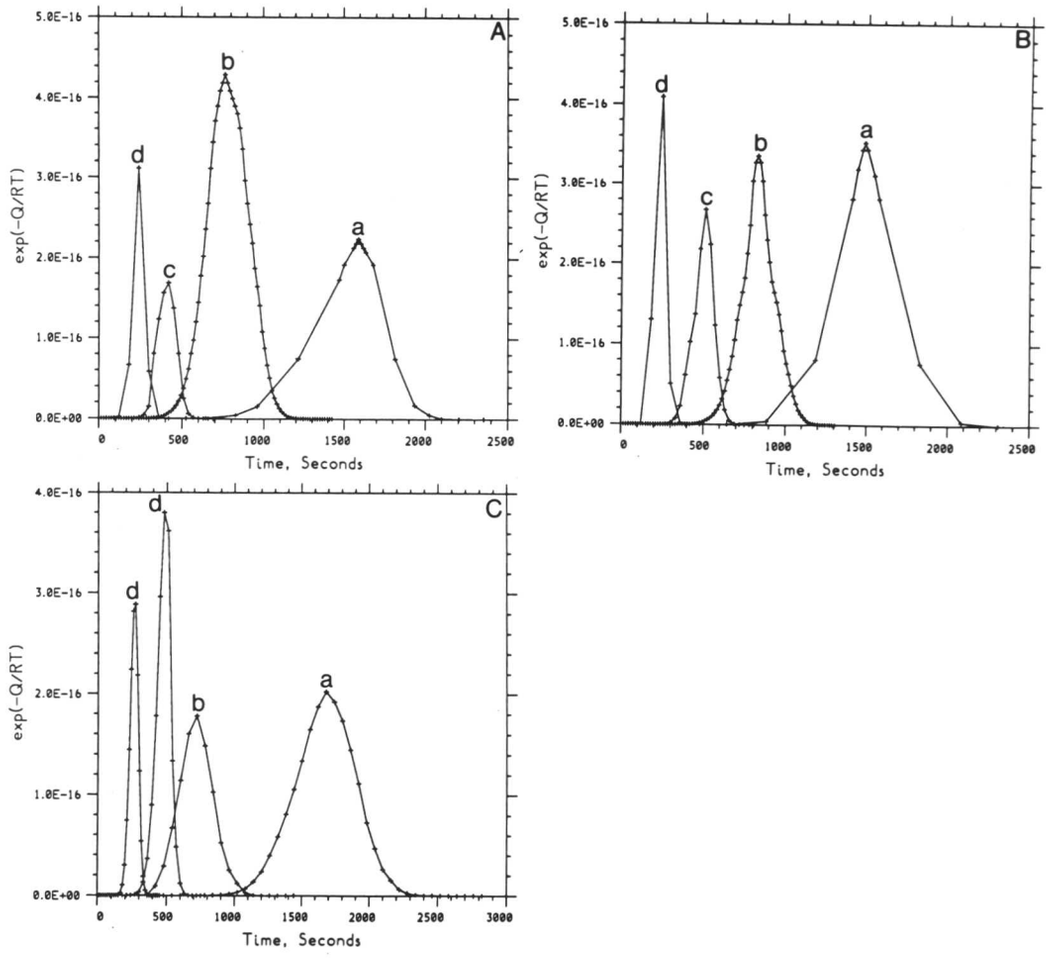

Figure 7.15(i). Showing the variation of kinetic strength exp(-Q/RT) versus time in seconds, where the value of Q = 654257 J mol^{-1}. Graphs A - C are for the specimens zone annealed in the as-received condition, after pre-annealing at 550°C for 90 hours and 10 days respectively.

Figure	T_p	Profiles	Specimen travel speeds mm/min.
7.15iA.	1150°C	a - d	0.8, 1.4, 3.2 and 5.0
7.15iB.	1150°C	a - d	0.8, 1.4, 3.2 and 5.0
7.15iC.	1150°C	a - d	0.8, 1.4, 3.2 and 5.0

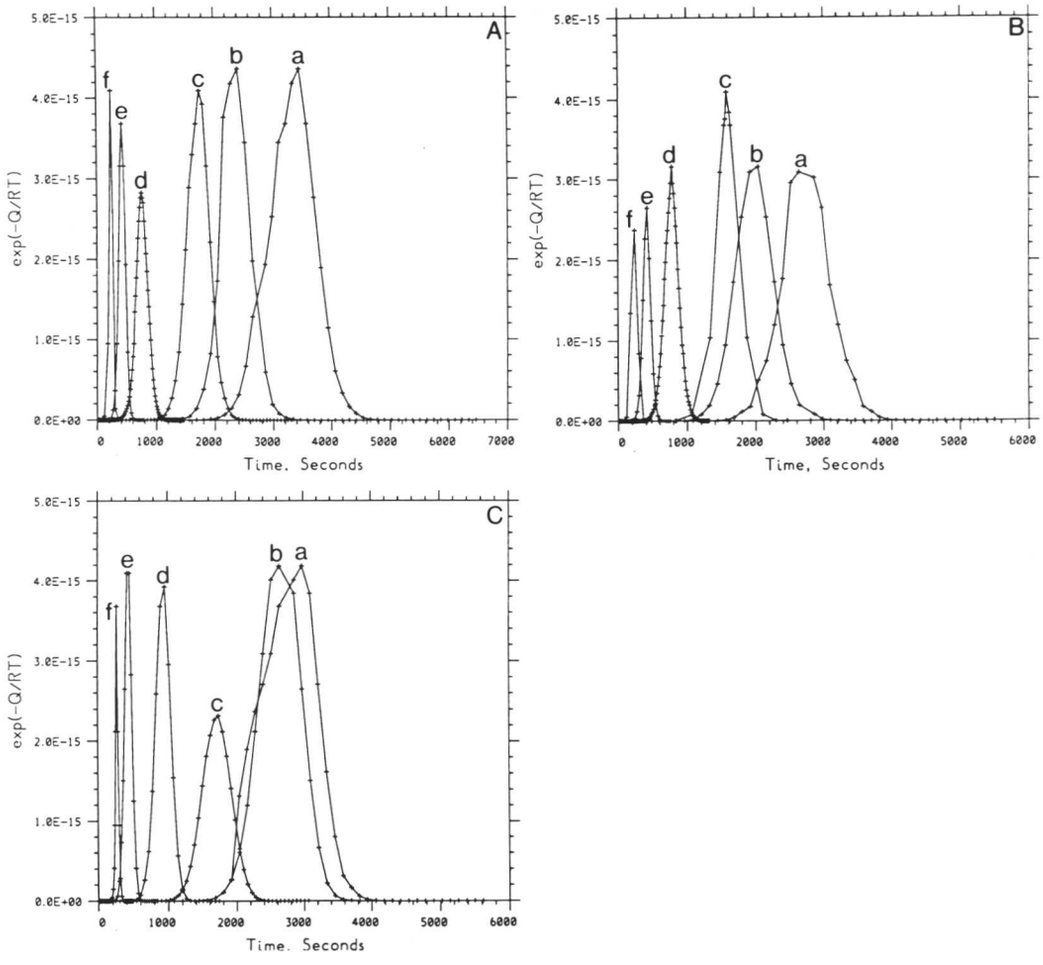

Figure 7.15(ii). Showing the variation of kinetic strength exp(-Q/RT) versus time in seconds, where the value of Q = 654257 J mol^{-1}. Graphs A - C are for the specimens zone annealed in the as-received condition, after pre-annealing at 550°C for 90 hours and 10 days respectively.

Figure	T_p	Profiles	Specimen travel speeds mm/min.
7.15iiA.	1250°C	a - f	0.2, 0.4, 0.8, 1.4, 3.2 and 5.0
7.15iiB.	1250°C	a - f	0.2, 0.4, 0.8, 1.4, 3.2 and 5.0
7.15iiC.	1250°C	a - f	0.2, 0.4, 0.8, 1.4, 3.2 and 5.0

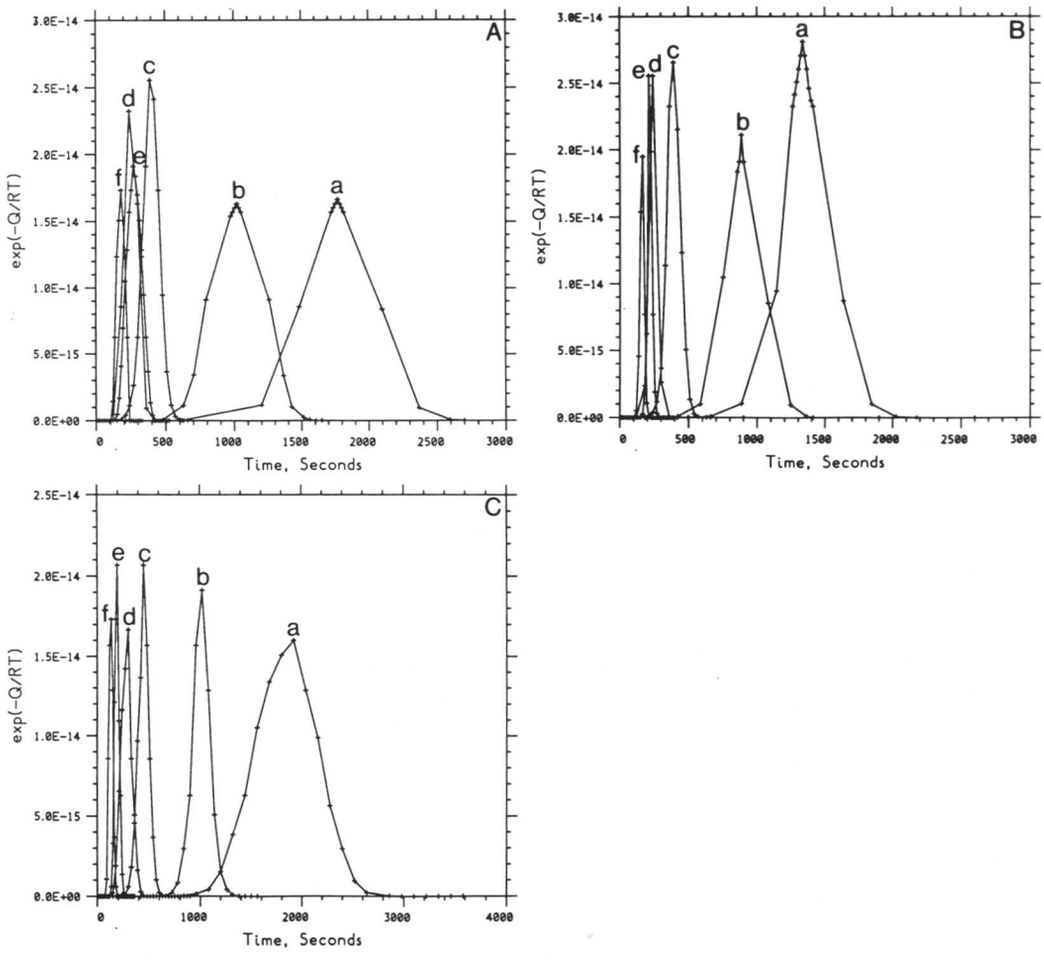

Figure 7.15(iii). Showing the variation of kinetic strength exp(-Q/RT) versus time in seconds, where the value of Q = 654257 J mol^{-1}. Graphs A - C are for the specimens zone annealed in the as-received condition, after pre-annealing at 550°C for 90 hours and 10 days respectively.

Figure	T_p	Profiles	Specimen travel speeds mm/min.
7.15iiiA.	1350°C	a - f	0.8, 1.4, 3.2, 5.0, 7.7 and 10.0
7.15iiiB.	1350°C	a - f	0.8, 1.4, 3.2, 5.0, 7.7 and 10.0
7.15iiiC.	1350°C	a - f	0.8, 1.4, 3.2, 5.0, 7.7 and 10.0

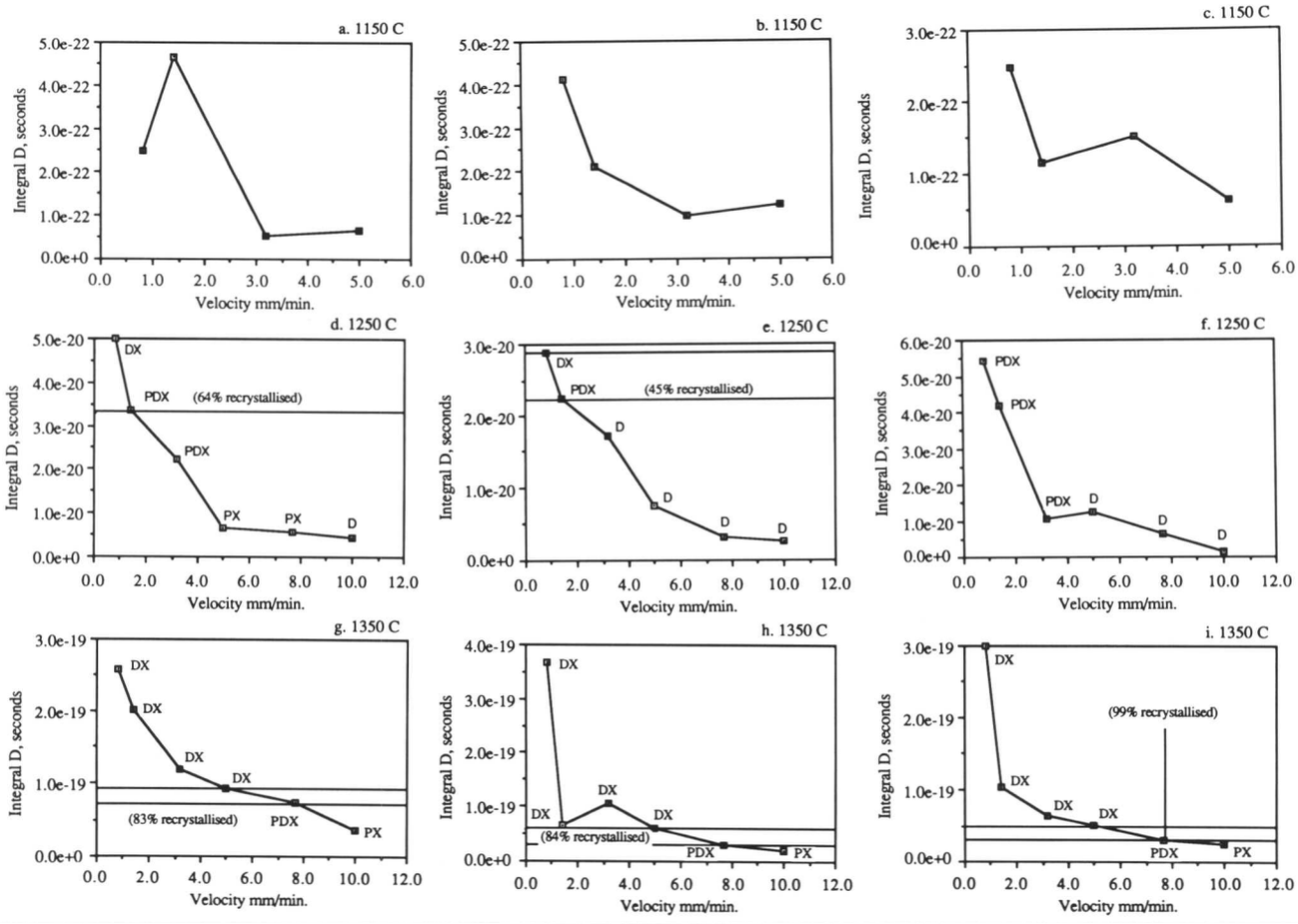

Figure 7.16. Showing the graphs plotted for integral D, seconds versus velocity mm/min. D (area under the curve) calculated with measured value of Q (i.e., 654257 J mol^{-1}).

Graphs	specimen condition
a, d & g	zone annealed in as-received condition
b, e & h	zone annealed after pre-annealing at 550°C for 90 hours
c, f & i	zone annealed after pre-annealing at 550°C for 10 days.

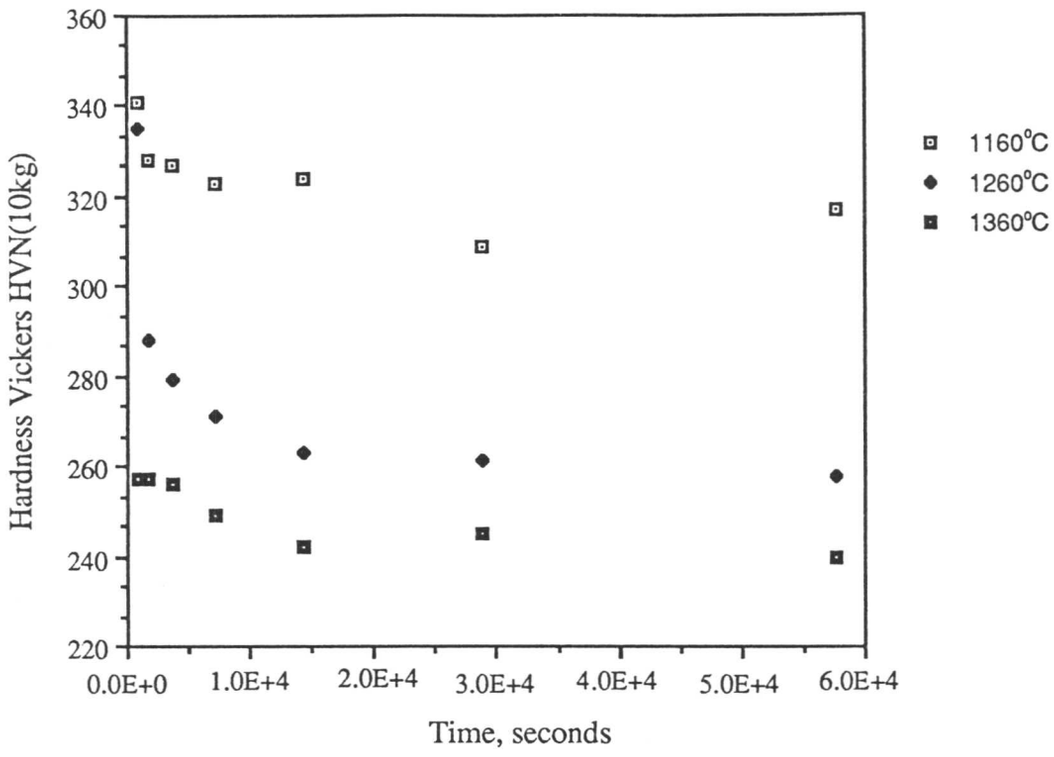

Figure 7.17. Graph showing the variation in hardness HVN(10kg) versus time in seconds after isothermal annealing MA957 at temperatures ranging from 1160 to 1360°C.

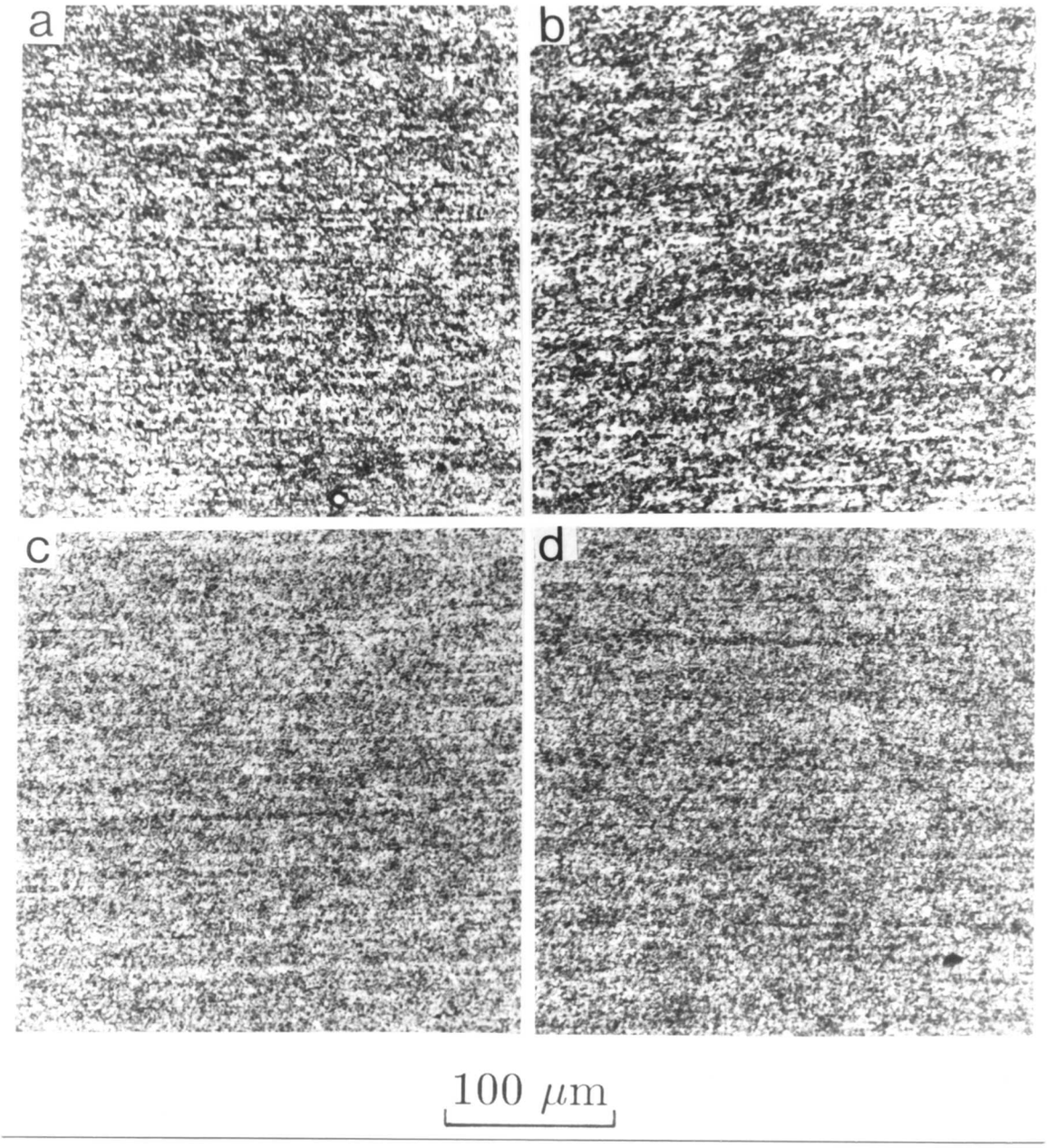

Figure 7.18. Optical micrographs illustrating the microstructure recorded after isothermal annealing at 1160°C for:

a. 900 seconds
b. 3600 seconds
c. 14400 seconds
d. 57600 seconds

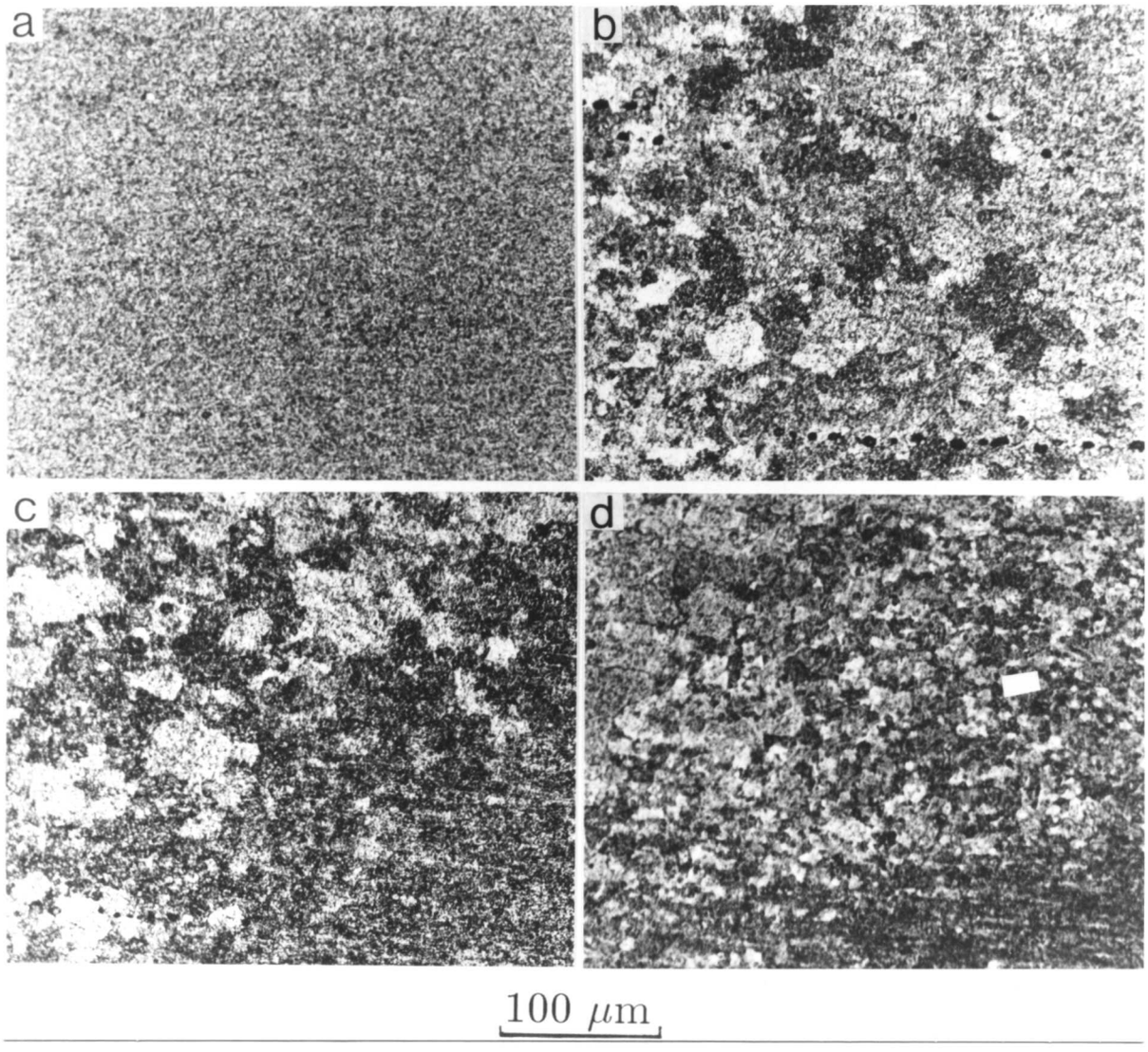

Figure 7.19. Micrographs showing the microstructure observed after isothermal annealing MA957 at 1260°C for:

a. 7200 seconds
b. 14400 seconds
c. 28800 seconds
d. 57600 seconds

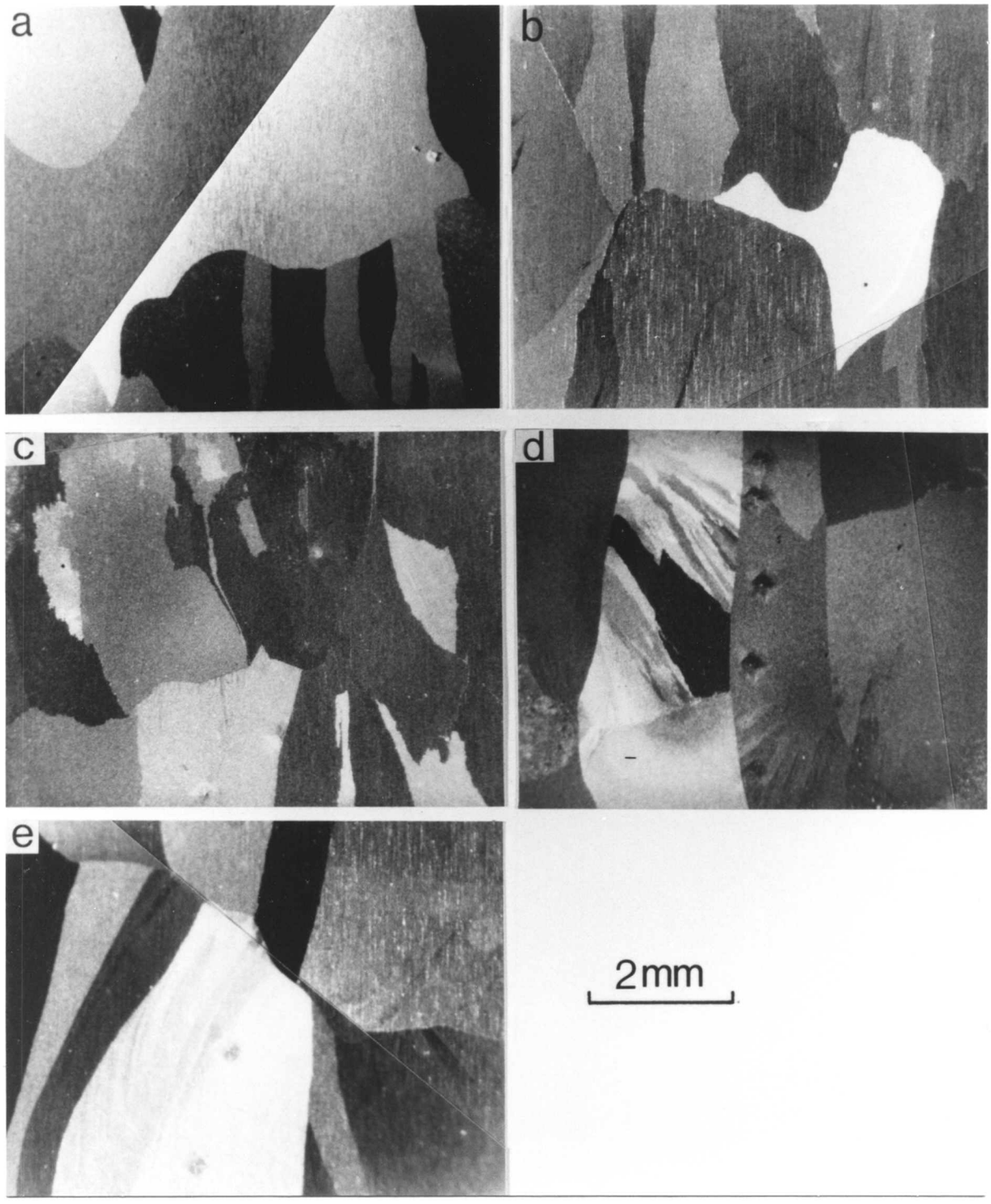

Figure 7.20. Showing the micrographs taken after isothermal annealing specimens of alloy MA957 at 1360°C for:

a. 3600 seconds
b. 7200 seconds
c. 14400 seconds
d.28800 seconds
e. 57600 seconds

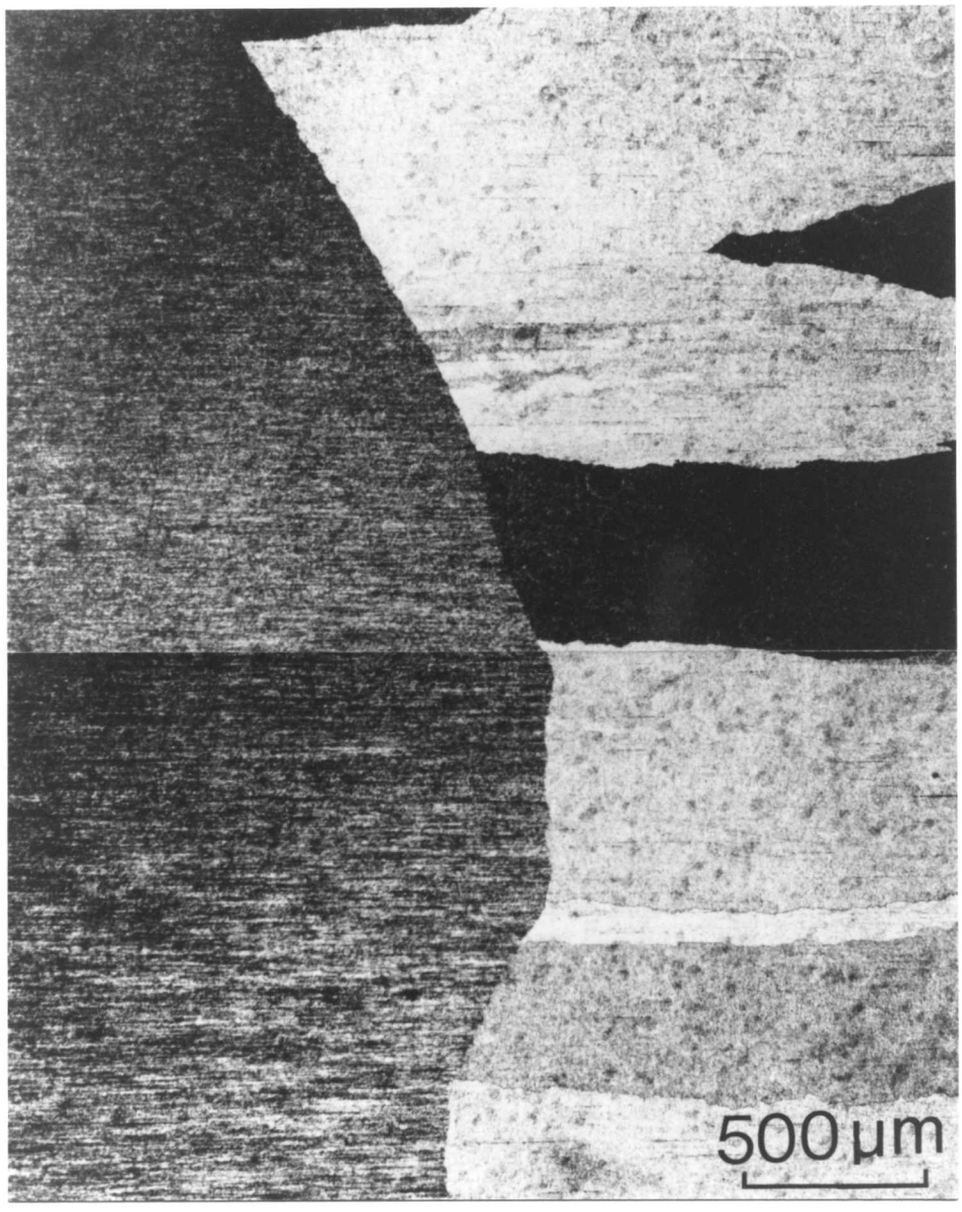

Figure 7.21. Optical micrograph representing the partially recrystallised region from the sample isothermally annealed at 1350°C for 3600 seconds (also see figure 7.20a).